Bonn-Gatchina partial wave analysis

A. Sarantsev

Petersburg Nuclear Physics Institute

HISKP (Bonn), PNPI (Russia)

The EBAC meeting

May 24-26 2010; JLab, United States

Bonn-Gatchina partial wave analysis group:

A. Anisovich, E. Klempt, V. Nikonov, A. Srantsev, U. Thoma

http://pwa.hiskp.uni-bonn.de/

Petersburg Nuclear Physics Institute

Bonn-Gatchina Partial Wave Analysis

Address: Nussallee 14-16, D-53115 Bonn Fax: (+49) 228 / 73-2505

Data Base | Meson Spectroscopy | Baryon Spectroscopy | NN-interaction | Formalism

Analysis of Other Groups	BG PWA	Useful Links
SAID	Publications	SPIRES
MAID	Talks	PDG Homepage
Giessen Uni	Contacts	Durham Data Base
		Bonn Homepage

CB-ELSA Homepage

Responsible: Dr. V. Nikonov, E-mail: *nikonov@hiskp.uni-bonn.de*
Last changes: January 26th, 2010.

Data Base

Pion induced reactions (χ^2 analysis).

Observable	$N_{\rm data}$	$\frac{\chi^2}{N_{\rm data}}$		Observable	$N_{\rm data}$	$\frac{\chi^2}{N_{\rm data}}$	
$N^*_{1/2-}$ $S_{11}(\pi N\to\pi N)$	104	1.81	SAID	$\Delta_{1/2-}$ $S_{31}(\pi N\to\pi N)$	112	2.27	SAID
$N^*_{1/2+}$ $P_{11}(\pi N\to\pi N)$	112	2.49	SAID	$\Delta_{1/2+}$ $P_{31}(\pi N\to\pi N)$	104	2.01	SAID
$N^*_{3/2+}$ $P_{13}(\pi N\to\pi N)$	112	1.90	SAID	$\Delta^*_{3/2+}$ $P_{33}(\pi N\to\pi N)$	120	2.53	SAID
$\Delta^*_{3/2-}$ $D_{33}(\pi N\to\pi N)$	108	2.56	SAID	$N^*_{3/2-}$ $D_{13}(\pi N\to\pi N)$	96	2.16	SAID
$N^*_{5/2-}$ $D_{15}(\pi N\to\pi N)$	96	3.37	SAID	$\Delta_{5/2+}$ $F_{35}(\pi N\to\pi N)$	62	1.32	SAID
$\Delta_{7/2+}$ $F_{37}(\pi N\to\pi N)$	72	2.86	SAID				
$d\sigma/d\Omega(\pi^-p\to n\eta)$	70	1.96	Richards *et al.*	$d\sigma/d\Omega(\pi^-p\to n\eta)$	84	2.67	CBALL
$d\sigma/d\Omega(\pi^-p\to K\Lambda)$	598	1.68	RAL	$P(\pi^-p\to K\Lambda)$	355	1.96	RAL+ANL
$d\sigma/d\Omega(\pi^+p\to K^+\Sigma)$	609	1.24	RAL	$P(\pi^+p\to K^+\Sigma)$	307	1.49	RAL
$d\sigma/d\Omega(\pi^-p\to K^0\Sigma^0)$	259	0.85	RAL	$P(\pi^-p\to K^0\Sigma^0)$	95	1.25	RAL

Data Base

π and η photoproduction reactions (χ^2 analysis).

Observable	$N_{\rm data}$	$\frac{\chi^2}{N_{\rm data}}$		Observable	$N_{\rm data}$	$\frac{\chi^2}{N_{\rm data}}$	
$d\sigma/d\Omega(\gamma p \to p\pi^0)$	1106	1.34	CB-ELSA	$d\sigma/d\Omega(\gamma p \to p\pi^0)$	861	1.46	GRAAL
$d\sigma/d\Omega(\gamma p \to p\pi^0)$	592	2.11	CLAS	$d\sigma/d\Omega(\gamma p \to p\pi^0)$	1692	1.25	TAPS@MAMI
$E(\gamma p \to p\pi^0)$	140	1.23	A2-GDH	$\Sigma(\gamma p \to p\pi^0)$	1492	3.26	SAID db
$P(\gamma p \to p\pi^0)$	607	3.23	SAID db	$T(\gamma p \to p\pi^0)$	389	3.71	SAID db
$H(\gamma p \to p\pi^0)$	71	1.26	SAID db	$G(\gamma p \to p\pi^0)$	75	1.50	SAID db
$O_x(\gamma p \to p\pi^0)$	7	1.77	SAID db	$O_z(\gamma p \to p\pi^0)$	7	0.46	SAID db
$d\sigma/d\Omega(\gamma p \to n\pi^+)$	1583	1.64	SAID db	$d\sigma/d\Omega(\gamma p \to n\pi^+)$	408	0.62	A2-GDH
$\Sigma(\gamma p \to n\pi^+)$	899	3.48	SAID db	$E(\gamma p \to n\pi^+$	231	1.55	A2-GDH
$P(\gamma p \to n\pi^+)$	252	2.90	SAID db	$T(\gamma p \to n\pi^+)$	661	3.21	SAID db
$H(\gamma p \to p\pi^+)$	71	3.90	SAID db	$G(\gamma p \to p\pi^+)$	86	5.64	SAID db
$d\sigma/d\Omega(\gamma p \to p\eta)$	680	1.47	CB-ELSA	$d\sigma/d\Omega(\gamma p \to p\eta)$	100	2.16	TAPS
$\Sigma(\gamma p \to p\eta)$	51	2.26	GRAAL 98	$\Sigma(\gamma p \to p\eta)$	100	2.02	GRAAL 07
$T(\gamma p \to p\eta)$	50	1.48	Phoenics				

Data Base

Kaon photoproduction (χ^2 analysis).

Observable	$N_{\rm data}$	$\frac{\chi^2}{N_{\rm data}}$		Observable	$N_{\rm data}$	$\frac{\chi^2}{N_{\rm data}}$	
$C_x(\gamma p \to \Lambda K^+)$	160	1.23	CLAS	$C_x(\gamma p \to \Sigma^0 K^+)$	94	2.20	CLAS
$C_z(\gamma p \to \Lambda K^+)$	160	1.41	CLAS	$C_z(\gamma p \to \Sigma^0 K^+)$	94	2.00	CLAS
$d\sigma/d\Omega(\gamma p \to \Lambda K^+)$	1320	0.81	CLAS09	$d\sigma/d\Omega(\gamma p \to \Sigma^0 K^+)$	1280	2.06	CLAS
$P(\gamma p \to \Lambda K^+)$	1270	2.21	CLAS09	$P(\gamma p \to \Sigma^0 K^+)$	95	1.45	CLAS
$\Sigma(\gamma p \to \Lambda K^+)$	66	1.53	GRAAL	$\Sigma(\gamma p \to \Sigma^0 K^+)$	42	0.90	GRAAL
$\Sigma(\gamma p \to \Lambda K^+)$	45	1.65	LEP	$\Sigma(\gamma p \to \Sigma^0 K^+)$	45	1.11	LEP
$T(\gamma p \to \Lambda K^+)$	66	1.26	GRAAL 09	$d\sigma/d\Omega(\gamma p \to \Sigma^+ K^0)$	48	3.76	CLAS
$O_x(\gamma p \to \Lambda K^+)$	66	1.30	GRAAL 09	$O_z(\gamma p \to \Lambda K^+)$	66	1.54	GRAAL 09
$d\sigma/d\Omega(\gamma p \to \Sigma^+ K^0)$	72	0.74	CB-ELSA 10	$P(\gamma p \to \Sigma^+ K^0)$	24	1.06	CB-ELSA 10
$\Sigma(\gamma p \to \Sigma^+ K^0)$	15	1.13	CB-ELSA 10				

Data Base

Multi-meson final states (maximum likelihood analysis).

$d\sigma/d\Omega(\pi^- p \to n\pi^0\pi^0)$	CBALL				
$\mathrm{d}\sigma/\mathrm{d}\Omega(\gamma\mathrm{p}\to\mathrm{p}\pi^0\pi^0)$	CB-ELSA (1.4 GeV)	$\mathrm{E}(\gamma\mathrm{p}\to\mathrm{p}\pi^0\pi^0)$	16	1.91	MAMI
$\mathrm{d}\sigma/\mathrm{d}\Omega(\gamma\mathrm{p}\to\mathrm{p}\pi^0\eta)$	CB-ELSA (3.2 GeV)	$\Sigma(\gamma\mathrm{p}\to\mathrm{p}\pi^0\eta)$	180	2.37	GRAAL
$\mathrm{d}\sigma/\mathrm{d}\Omega(\gamma\mathrm{p}\to\mathrm{p}\pi^0\pi^0)$	CB-ELSA (3.2 GeV)	$\Sigma(\gamma\mathrm{p}\to\mathrm{p}\pi^0\pi^0)$	128	0.96	GRAAL
$\mathrm{d}\sigma/\mathrm{d}\Omega(\gamma\mathrm{p}\to\mathrm{p}\pi^0\eta)$	CB-ELSA (3.2 GeV)	$\Sigma(\gamma\mathrm{p}\to\mathrm{p}\pi^0\eta)$	180	2.37	GRAAL
$\mathrm{I_c}(\gamma\mathrm{p}\to\mathrm{p}\pi^0\eta)$	CB-ELSA (3.2 GeV)	$\mathrm{I_s}(\gamma\mathrm{p}\to\mathrm{p}\pi^0\eta)$	CB-ELSA (3.2 GeV)		

Energy dependent approach

In many cases an unambiguous partial wave decomposition at fixed energies is impossible. Then the energy and angular parts should be analyzed together:

$$A(s,t) = \sum_{\beta\beta' n} A_n^{\beta\beta'}(s) Q^{(\beta)+}_{\mu_1\ldots\mu_n} F^{\mu_1\ldots\mu_n}_{\nu_1\ldots\nu_n} Q^{(\beta')}_{\nu_1\ldots\nu_n}$$

1. **C. Zemach, Phys. Rev. 140, B97 (1965); 140, B109 (1965).**
2. **S.U.Chung, Phys. Rev. D 57, 431 (1998).**
3. **A.V. Anisovich** *et al.* **J. Phys. G 28 15 (2002)**

   V. V. Anisovich, M. A. Matveev, V. A. Nikonov, J. Nyiri and A. V. Sarantsev,

   Hackensack, USA: World Scientific (2008) 580 p

1. **Correlations between angular part and energy part are under control.**
2. **Unitarity and analyticity can be introduced from the beginning.**
3. **However, to fix simultaneously energy and angular dependencies of the amplitude a combined fit of many reactions is needed.**

Resonance amplitudes for meson photoproduction

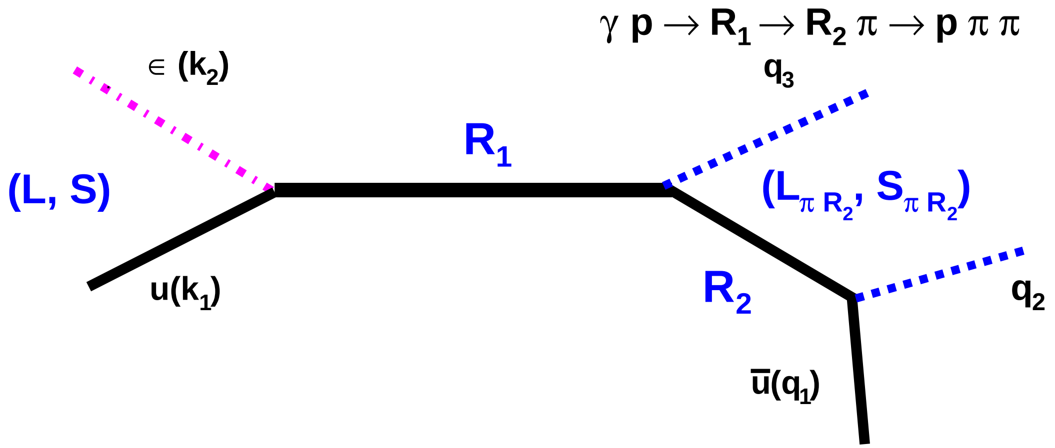

General form of the angular dependent part of the amplitude:

$$\bar{u}(q_1)\tilde{N}_{\alpha_1\ldots\alpha_n}(R_2\to\mu N)F^{\alpha_1\ldots\alpha_n}_{\beta_1\ldots\beta_n}(q_1+q_2)\tilde{N}^{(j)\beta_1\ldots\beta_n}_{\gamma_1\ldots\gamma_m}(R_1\to\mu R_2)$$
$$F^{\gamma_1\ldots\gamma_m}_{\xi_1\ldots\xi_m}(P)V^{(i)\mu}_{\xi_1\ldots\xi_m}(R_1\to\gamma N)u(k_1)\varepsilon_\mu$$

$$F^{\mu_1\ldots\mu_L}_{\nu_1\ldots\nu_L}(p)=(m+\hat{p})O^{\mu_1\ldots\mu_L}_{\alpha_1\ldots\alpha_L}\frac{L+1}{2L+1}\left(g^{\perp}_{\alpha_1\beta_1}-\frac{L}{L+1}\sigma_{\alpha_1\beta_1}\right)\prod_{i=2}^{L}g_{\alpha_i\beta_i}O^{\beta_1\ldots\beta_L}_{\nu_1\ldots\nu_L}$$

$$\sigma_{\alpha_i\alpha_j}=\frac{1}{2}(\gamma_{\alpha_i}\gamma_{\alpha_j}-\gamma_{\alpha_j}\gamma_{\alpha_i})$$

The simplest parameterization of the pole contribution:

The Breit-Wigner amplitude

$$A_{a\to b}=\frac{g_a g_b}{M^2-s-i\sum\limits_j \rho_j(s) g_j^2}$$

where g_j are couplings and $\rho_j(s)$ are phase volumes.

The width of the state is formed by decays into fitted channels: πN, ηN, $K\Lambda$, $K\Sigma$, $\pi\Delta$, $N\sigma$, $P_{11}(1440)\pi$, $D_{13}(1520)\pi$,... and an additional width, defined by the decay into $N\rho(770)$.

The photoproduction amplitude:

$$A_{\gamma p\to b}=\frac{g_{\gamma p} g_b}{M^2-s-i\sum\limits_j \rho_j(s) g_j^2}$$

Two body phase volume:

$$\rho(s,m_1,m_2) = \frac{2k}{\sqrt{s}}\frac{k^{2L}}{F(L,k^2,r)}\frac{m_1+k_0}{2m_1}\;\frac{1.5-s_0}{s-s_0}$$

$$\frac{2k}{\sqrt{s}} = \frac{\sqrt{(s-(m_1+m_2)^2)(s-(m_1-m_2)^2)}}{s}$$

Here s is the invariant energy squared, m_1 is the baryon mass and m_2 is the meson mass. The Blatt-Weisskopf factor:

$$\begin{aligned}
F(L=0,k^2,r) &= 1\ , \\
F(L=1,k^2,r) &= (x+1)/r^2\ , \qquad\qquad x=k^2r^2 \\
F(L=2,k^2,r) &= (x^2+3x+9)/r^4\ , \\
F(L=3,k^2,r) &= (x^3+6x^2+45x+225)/r^6\ , \\
F(L=4,k^2,r) &= (x^4+10x^3+135x^2+1575x+11025)/r^8\ ,
\end{aligned} \tag{1}$$

where $r=0.8fm$ and L is the orbital momentum.

Three body phase volume:

$$\rho_3(s) = \int\limits_{(m_2+m_3)^2}^{(\sqrt{s}-m_1)^2} \frac{ds_{23}}{\pi} \frac{\rho(s,\sqrt{s_{23}},m_1)\, M_R\Gamma^R_{tot}}{(M_R^2-s_{23})^2+(M_R\Gamma^R_{tot})^2} \;,$$

$$M_R\Gamma^R_{tot} = \rho(s_{23},m_2,m_3)g^2(s_{23}) \;,$$

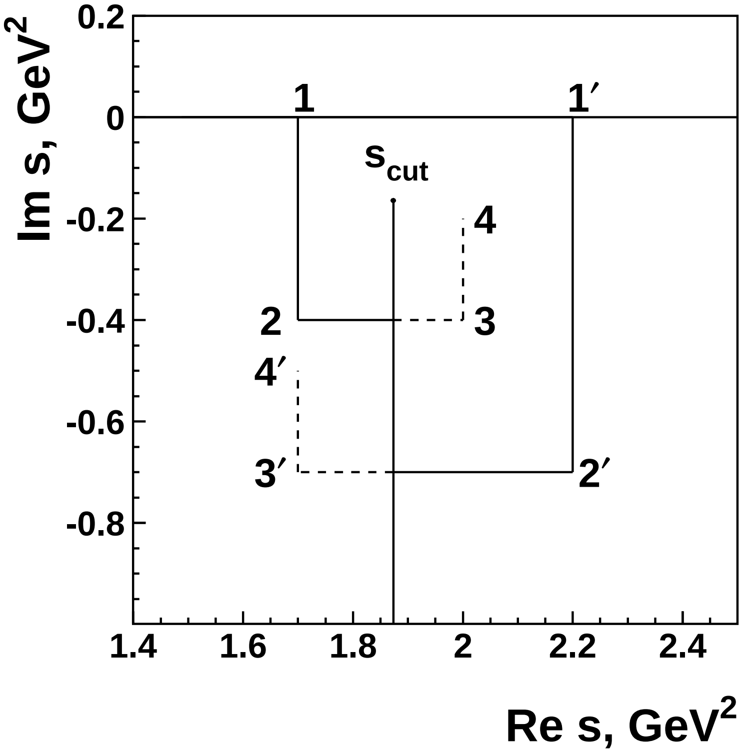

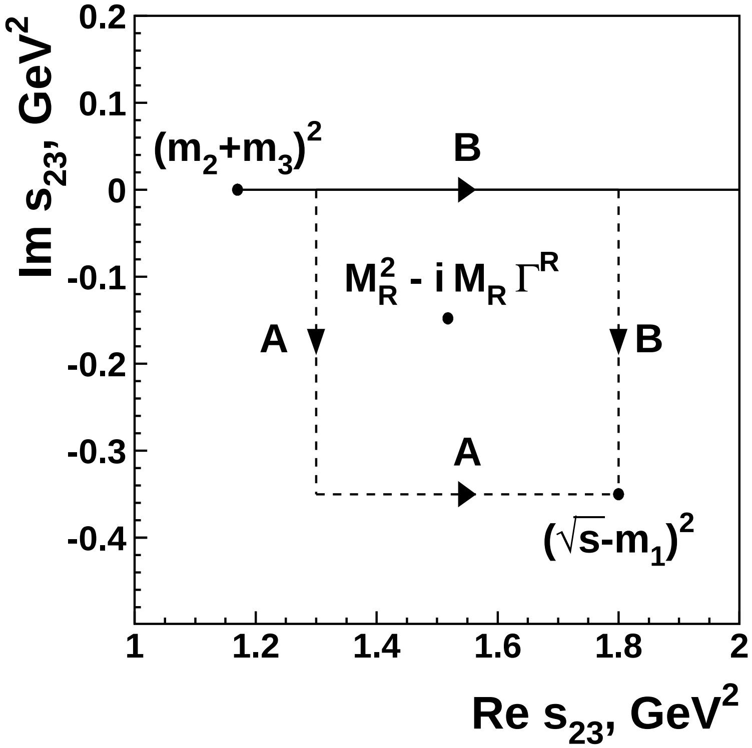

1 K-matrix representation of the scattering amplitude

The unitarity condition for the partial wave amplitude:

$$SS^{+} = I \qquad\qquad S = I + 2i\hat{\rho}(s)\hat{A}(s)$$

$$S = \frac{I + i\hat{\rho}\hat{K}}{I - i\hat{\rho}\hat{K}} = I + 2i\hat{\rho}A(s), \qquad\qquad A(s) = \hat{K}(I - i\hat{\rho}\hat{K})^{-1}$$

Where $\hat{K}$ is a real matrix.

One pole, multi-channel K-matrix corresponds to the relativistic Breit-Wigner amplitude:

$$K_{ab} = \frac{g_a g_b}{M^2 - s} \qquad \to \qquad A_{ab} = \frac{g_a g_b}{M^2 - s - i\sum\limits_j \rho_j(s) g_j^2}$$

For two poles:

$$K = \frac{g_1^2}{M_1^2 - s} + \frac{g_2^2}{M_2^2 - s}$$

$$A(s) = \frac{g_1^2(M_2^2-s) + g_2^2(M_1^2-s)}{(M_1^2-s)(M_2^2-s)-i\rho(s)\big(g_1^2(M_2^2-s) + g_2^2(M_1^2-s)\big)}$$

Compare with sum of two Breit-Wigner amplitudes:

$$A(s) = \frac{g_1^2(M_2^2-s) + g_2^2(M_1^2-s) - 2i\rho(s)g_1^2g_2^2}{(M_1^2-s)(M_2^2-s) - \rho^2(s)g_1^2g_2^2 - i\rho(s)\big(g_1^2(M_2^2-s) + g_2^2(M_1^2-s)\big)}$$

If in a fit we added a Breit-Wigner amplitude we allow couplings to have phases.

P-vector approach

The $\gamma\gamma \to \pi\pi$ reaction: the contribution from the $\gamma\gamma$-loop to the width of the state can be neglected.

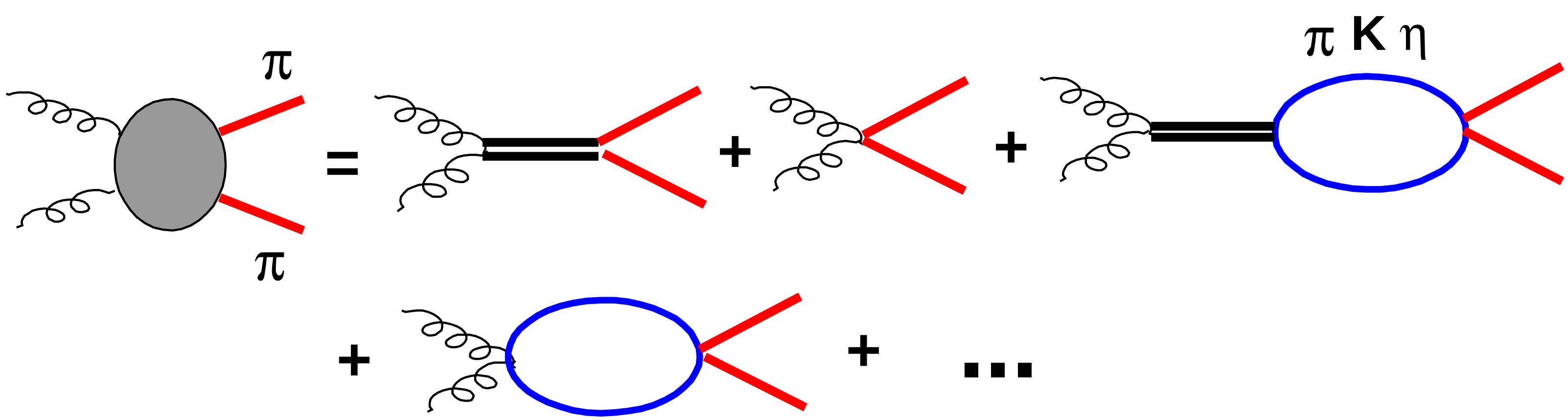

$$A_k = P_j (I - i\rho K)^{-1}_{jk} \qquad P_j = \sum_m \frac{\Lambda_n g_1^{(n)}}{M_n^2 - s} + F_j$$

Combined analysis of the different reactions:

For pion induced reactions the transition partial wave amplitude can be written as:

$$A_{1i} = K_{1j}(I - i\rho K)^{-1}_{ji}$$

and

$$K_{ij} = \sum_\alpha \frac{g_i^\alpha g_j^\alpha}{M_\alpha^2 - s} + f_{ij}(s) \qquad\qquad f_{ij} = \frac{f_{ij}^{(1)} + f_{ij}^{(2)}\sqrt{s}}{s - s_0^{ij}}\,.$$

where f_{ij} is nonresonant transition part.

For the photoproduction:

$$A_k = P_j(I - i\rho K)^{-1}_{jk}$$

The vector of the initial interaction has the form:

$$P_j = \sum_\alpha \frac{\Lambda^\alpha g_j^\alpha}{M_\alpha^2 - s} + F_j(s)$$

Here F_j is nonresonant production of the final state j.

Reggezied exchanges:

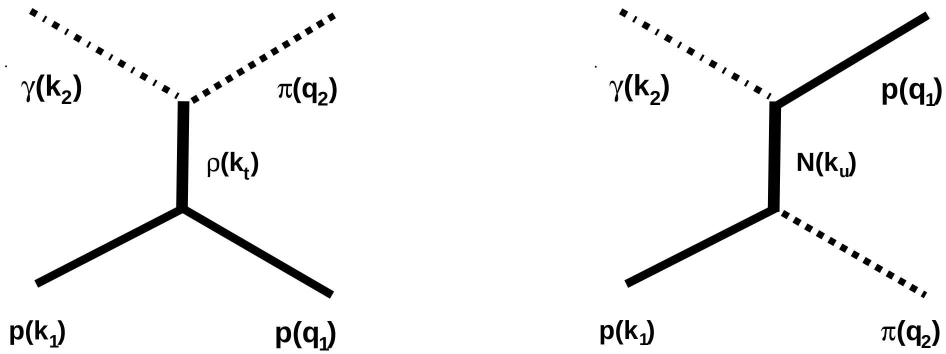

The amplitude for t-channel exchange:

$$A = g_1(t)g_2(t)R(\xi,\nu,t) = g_1(t)g_2(t)\frac{1+\xi exp(-i\pi\alpha(t))}{\sin(\pi\alpha(t))} \quad {\frac{\nu}{\nu_0}}^{\alpha(t)} \qquad \nu = \frac{1}{2}(s-u).$$

Here $\alpha(t)$ is the reggion trajectory, and ξ is its signature:

$$R(+,\nu,t) = \frac{e^{-i\frac{\pi}{2}\alpha(t)}}{\sin(\frac{\pi}{2}\alpha(t))\Gamma \quad \frac{\alpha(t)}{2}} \quad {\frac{\nu}{\nu_0}}^{\alpha(t)} ,$$

$$R(-,\nu,t) = \frac{ie^{-i\frac{\pi}{2}\alpha(t)}}{\cos(\frac{\pi}{2}\alpha(t))\Gamma \quad \frac{\alpha(t)}{2}+\frac{1}{2}} \quad {\frac{\nu}{\nu_0}}^{\alpha(t)} .$$

D-vector approach

For πN transition into channel 'a' the amplitude can be written as:

$$A_a \;=\; \hat{D}_a + [\hat{K}(\hat{I} \;-\; i\hat{\rho}\hat{K})^{-1}\,\hat{\rho}]_{ab}\hat{D}_b \;,$$

For strong channels:

$$D_a = K_{1a} \qquad A_a = K_{1j}(I - i\rho K)^{-1}_{ji}$$

For weak channels:

$$D_a = \sum_\alpha \frac{g_1^\alpha \Lambda_a^{dec}}{M_\alpha^2 - s} + d_{1a}(s)$$

For photoproduction of 'weak channels'

$$A_{ab} \;=\; \hat{G}_{ab} + \hat{P}_a(\hat{I} \;-\; i\hat{\rho}\hat{K})^{-1}\,\hat{\rho}\hat{D}_b \qquad G_{ab} = \sum_\alpha \frac{\Lambda_b \Lambda_a^{dec}}{M_\alpha^2 - s} + b_{ab}(s)$$

Production of three particle final states. Triangle singularities in the three particle system are logarithmic singularities.

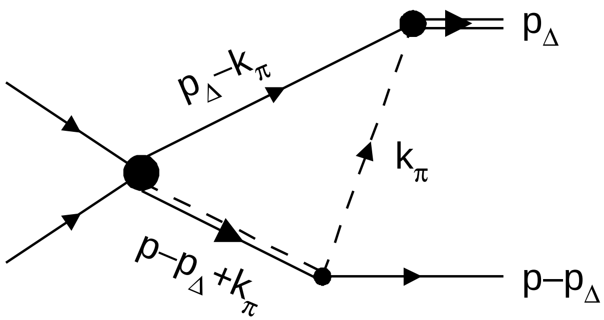

$$A^{\rm spinless}_{\rm triangle}(W^2,s)=\int\frac{d^4k_\pi}{i(2\pi)^4}\frac{1}{m_\pi^2-k_\pi^2-i0}$$
$$\times\frac{1}{m_\Delta^2-(p-p_\Delta+k_\pi)^2-im_\Delta\Gamma_\Delta}\frac{1}{m_N^2-(p_\Delta-k_\pi)^2-i0}$$

$$p=p_1+p_2,\quad p^2=W^2,\quad p_\Delta^2=s,\quad W_{min}=m_N+m_N+m_\pi.$$

The logarithmic singularity in most cases is weaker then the pole singularity. However it provides a complex vertex.

D-vector components for 3-particle final states should have phases. We allow them for resonance couplings and nonresonant terms

Description of $\pi\pi \to \pi\pi$, $\pi\pi \to \eta\eta$, $\pi\pi \to \eta\eta'$ and $\pi\pi \to K\bar{K}$ S-wave intensity (GAMS).

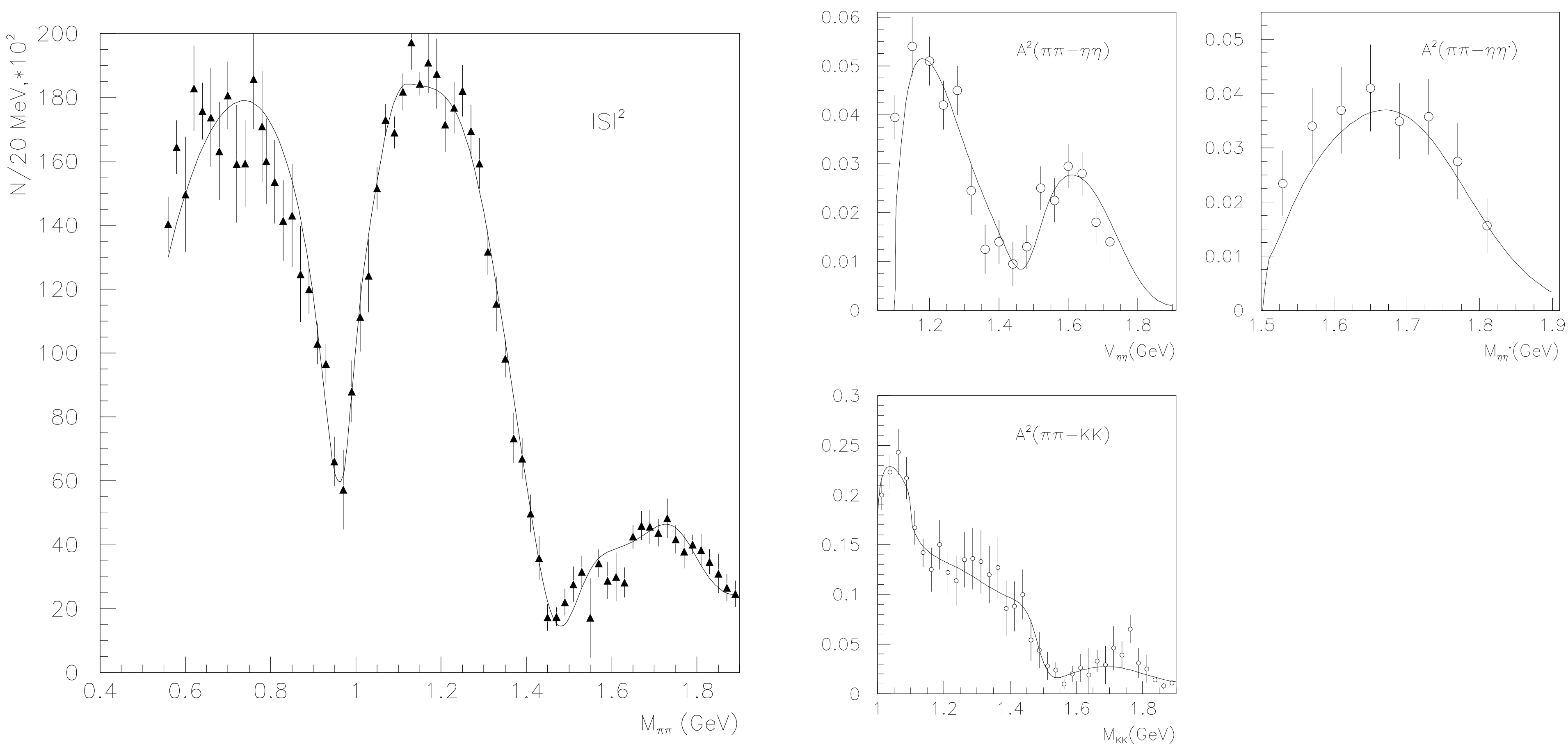

$$\bar{p}p \longrightarrow \pi^0\pi^0\pi^0$$

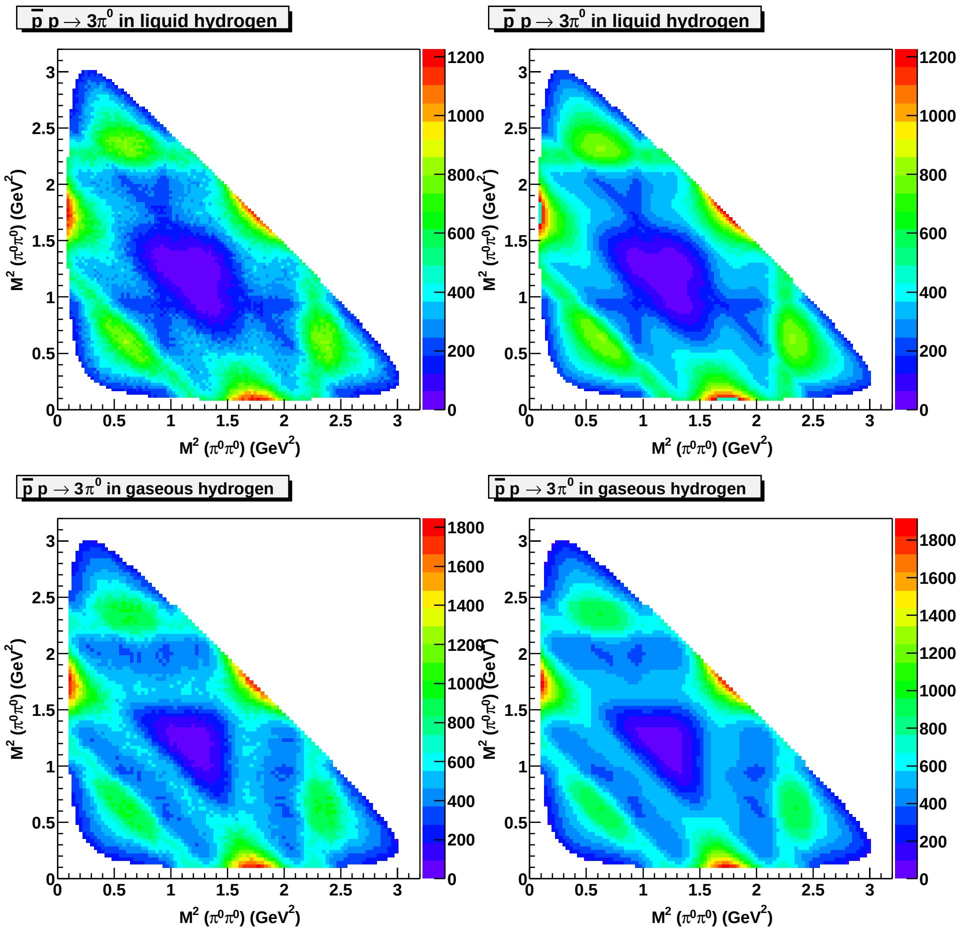

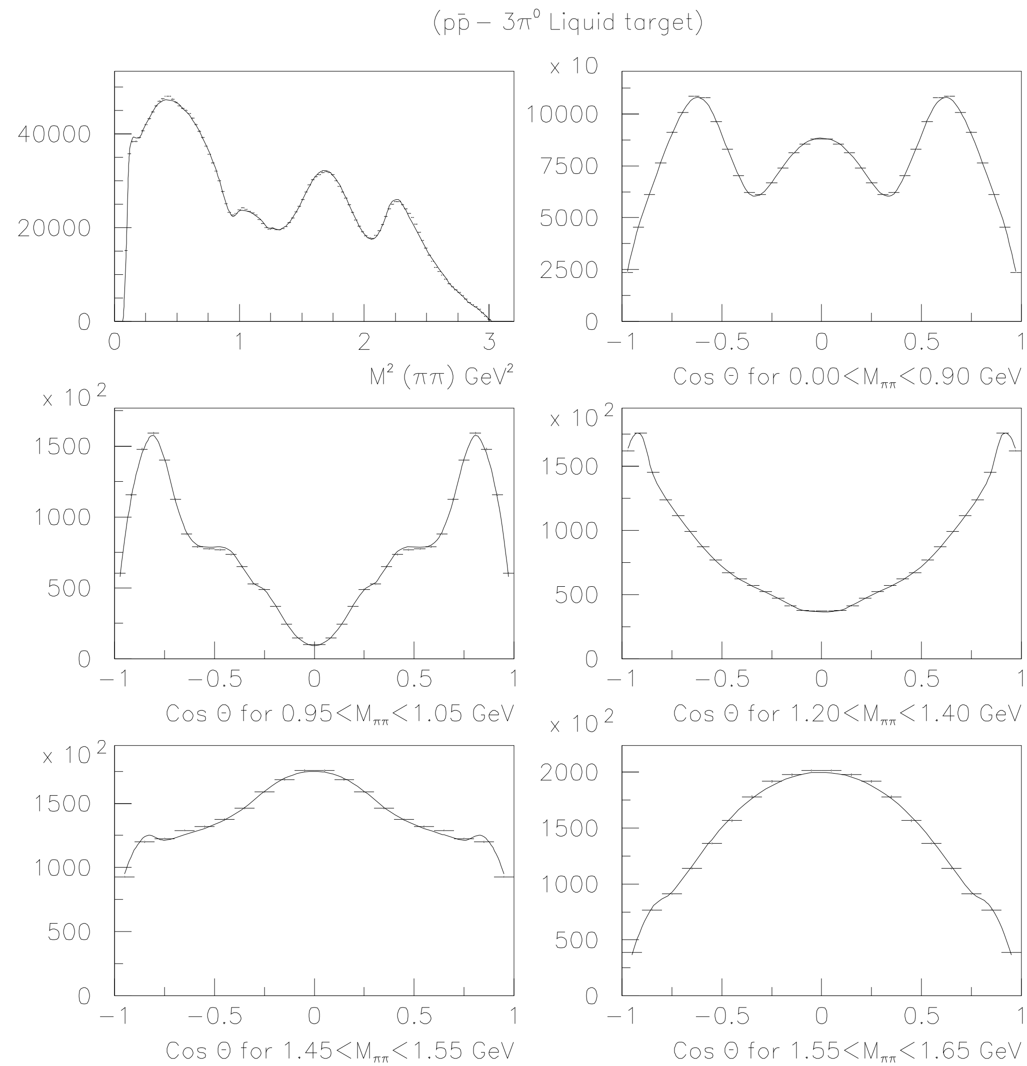

1. **K-matrix approach satisfies the unitarity condition. It takes into account right-hand side singularities of the amplitude: threshold singularities (cuts) and pole singularities.**
2. **The P-vector, D-vector and PD-methods allow us to perform of analysis of many reactions simultaneously.**
3. **This approach is fast enough to perform the analysis of modern high statistical data and reliably extract leading singularities of the amplitude. This is impossible with most approaches which solve directly integral (e.g. Bethe-Salpeter) equations.**

However:

This approach does not take into account correctly left-hand side singularities due to neglecting of real part of loop diagrams and therefore is not fully reliable at very low energies or in presence of strong thresholds

N/D based analysis of the data

In the case of resonance contributions only we have factorization and Bethe-Salpeter equation can be easily solved:

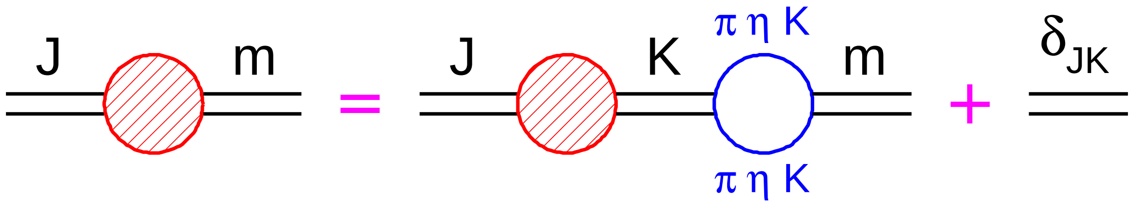

$$A_{jm} = A_{jk} \sum_{\alpha} B^{km}_{\alpha}(s) \frac{1}{M_m - s} + \frac{\delta_{jm}}{M_j^2 - s} \qquad B^{km}_{\alpha}(s) = \int\limits_{4m_j^2}^{\infty} \frac{ds'}{\pi} \frac{g^{(k)}_{\alpha}(s')\rho(s')g^{(m)}_{\alpha}(s')}{s' - s - i0}$$

$$\hat{A} = \hat{\kappa}(I - \hat{B}\hat{\kappa})^{-1} \qquad \kappa_{ij} = \frac{\delta_{ij}}{M_i^2 - s} \qquad B^{ij} = \sum_{\alpha} B^{km}_{\alpha}(s)$$

For non-resonant contributions: there is no factorization and the amplitude can have a complicated energy dependence. However in majority of K-matrix analysis the nonresonant contributions are constant or have a simple energy dependence. Non-factorization can be taken into account by introduction of two transitions with fixed left and right vertices.

Parameterization of P_{13} wave: 3 resonances 8 channels, 4 non-resonant contributions $\pi N \to \pi N$, $\pi N \to \eta N$, $\pi N \to K\Sigma$, $\pi N \to \Delta\pi$. It corresponds to 8×8 channel K-matrix and 5×5 N/D-matrix.

In many cases (fixed form-factor or subtraction procedure) the real part can be calculated in advance (for S-wave):

$$B(s) = ReB(M^2) + \frac{g^2}{\pi}[\rho(s)\; ln\frac{1-\rho(s)}{1+\rho(s)} - \rho(M^2)\; ln\frac{1-\rho(M^2)}{1+\rho(M^2)}] + i\rho(s)g^2$$

The P-vector approach is strait forward:

$A_{ab} = \sum_{ij}$ 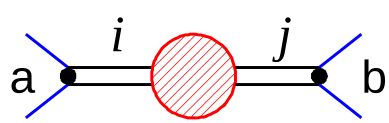

$P_b = \sum_{ij}$ 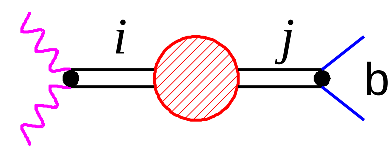

1. **This approach satisfies analyticity and two body unitarity conditions. It takes left-hand side singularities into account.**
2. **The approach is suitable for the analysis of high statistic data in combined analysis of many reactions.**
3. **However: a treatment of the real part for interfering resonances is model dependent.**

Bonn-Gatchina partial wave analysis.

1. **K-matrix:** $\pi N \to \pi N$, $\pi N \to \eta N$, $\pi N \to K\Lambda$ **and** $\pi N \to K\Sigma$ **reactions.**

   Included channels: πN, ηN, $K\Lambda$, $K\Sigma$, $\pi\Delta(1232)$, $N\sigma$, $N\rho$.

   First results for the S_{11} wave fitted in the N/D approach.

2. **P-vector:** $\gamma N \to \pi N$, $\gamma N \to \eta N$, $\gamma N \to K\Lambda$ **and** $\gamma N \to K\Sigma$ **reactions.**

   Preliminary fit with Reggee exchanges included in the P-vectors.

3. **D-vector:** $\pi N \to \pi\pi N$

4. **PD-approach** $\gamma N \to \pi\pi N$, $\gamma N \to \pi\eta N$

   D-vector channels: $P_{11}(1440)\pi$, $D_{13}(1520)\pi$, $F_{15}(1675)\pi$, $f_2(1275)N$, $\Delta\eta$,...

Fit of the SAID energy fixed solution for πN elastic partial waves

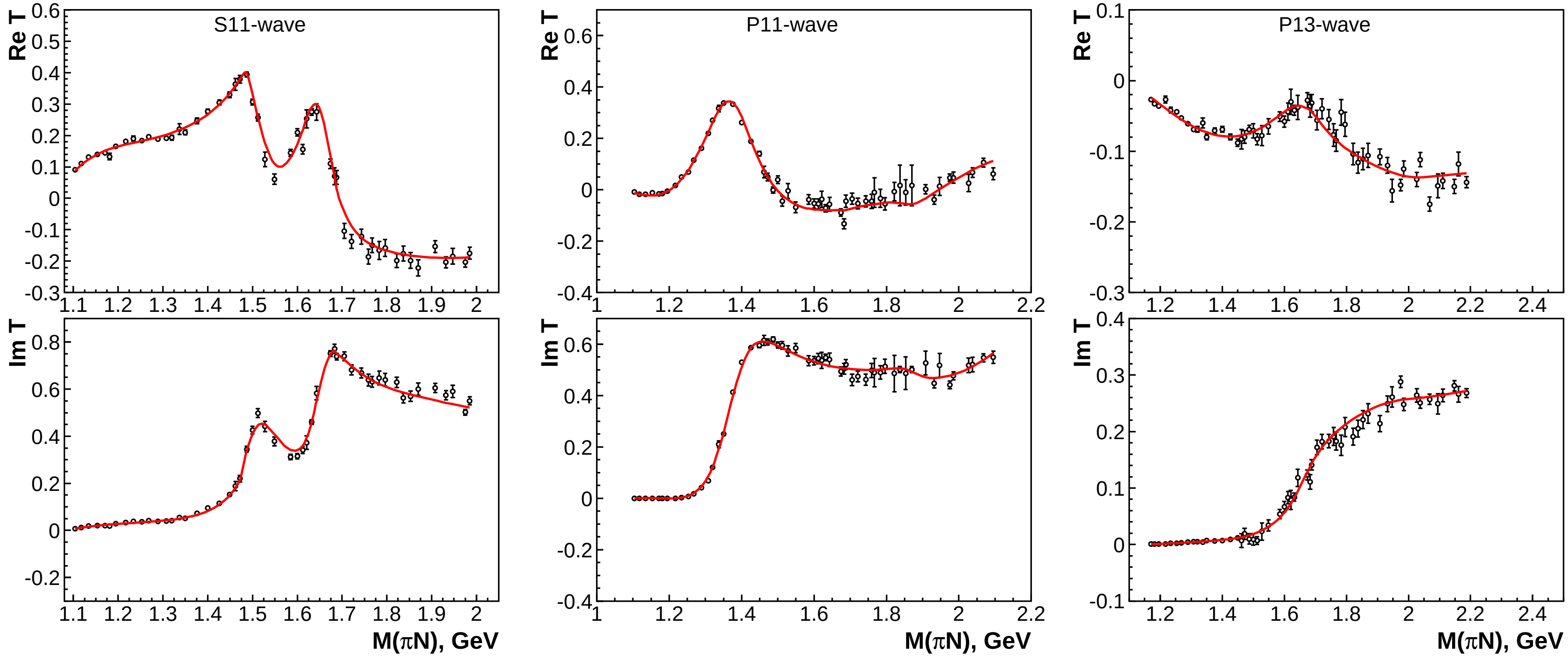

Fit of the SAID energy fixed solution for πN elastic partial waves

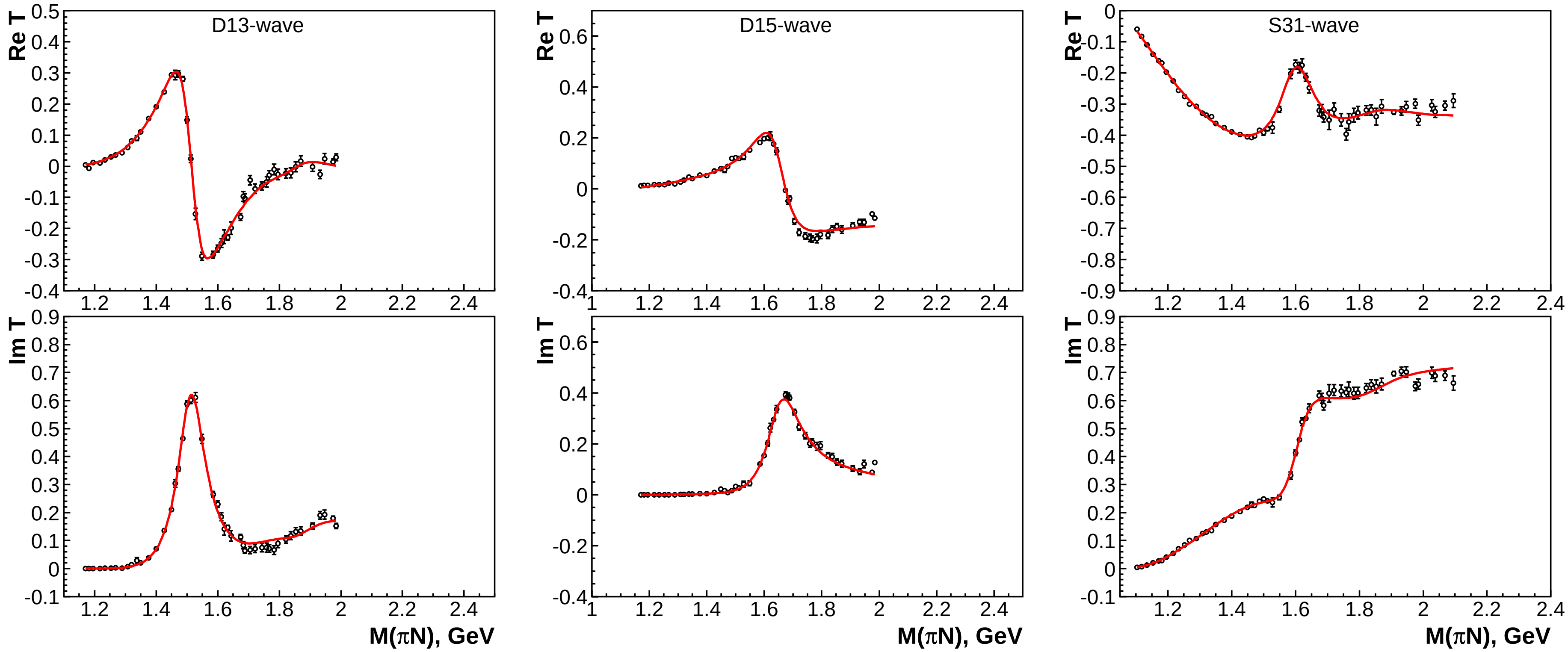

Fit of the SAID energy fixed solution for πN elastic partial waves

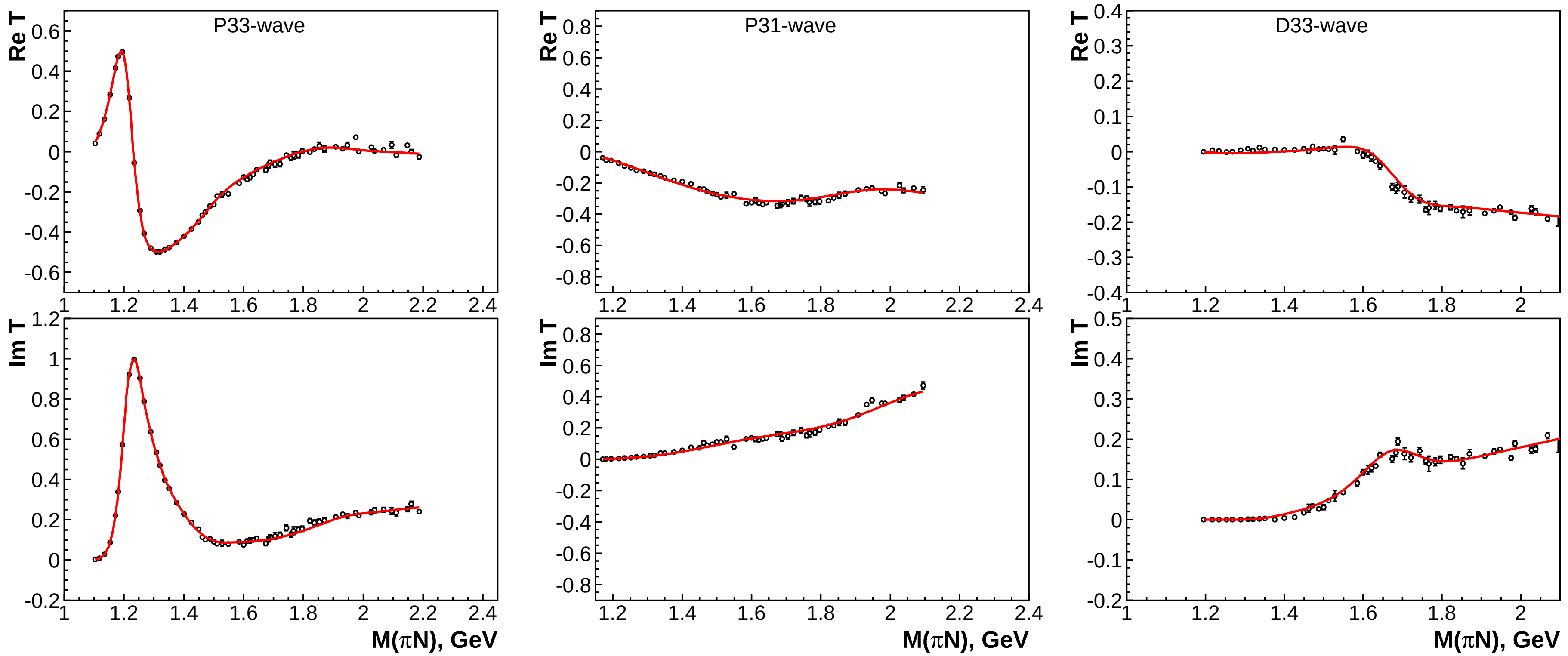

Fit of the SAID energy fixed solution for πN elastic partial waves

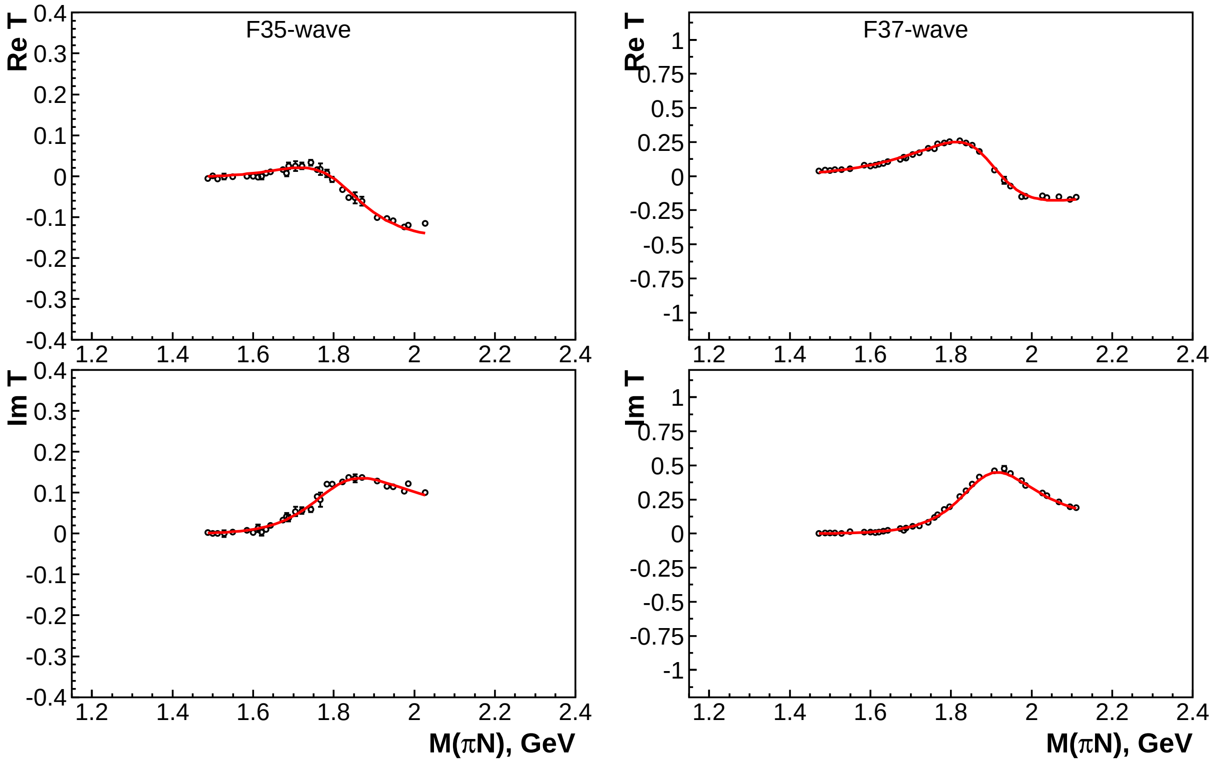

The fit of the the $\pi^- p \to K\Lambda$ reaction

The $P_{11}(1710)$ and $P_{13}(1900)$ states

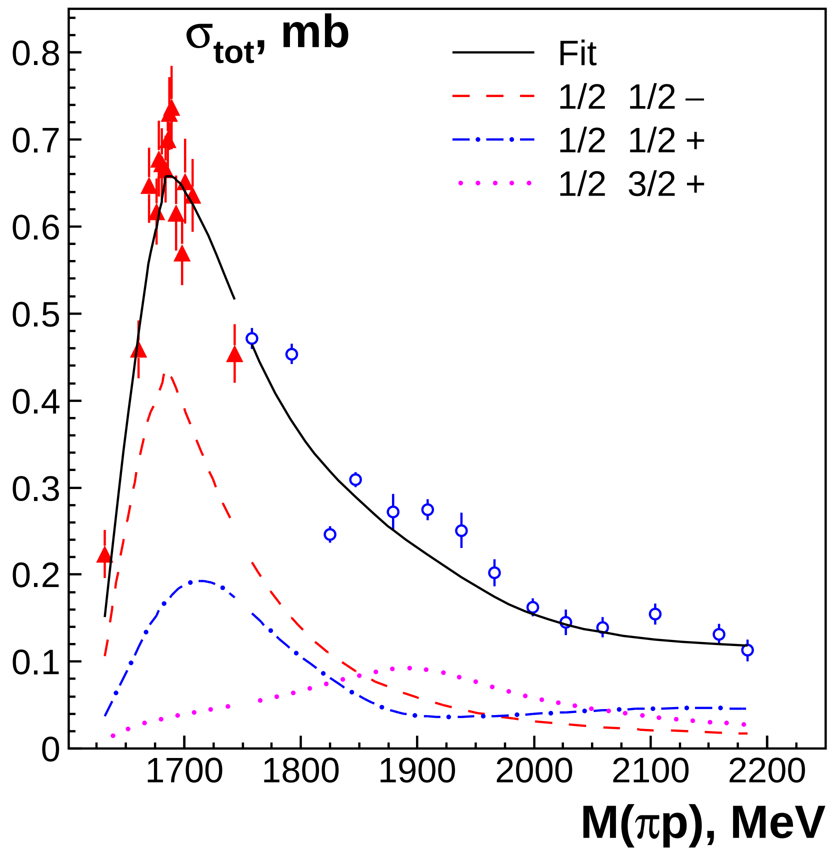

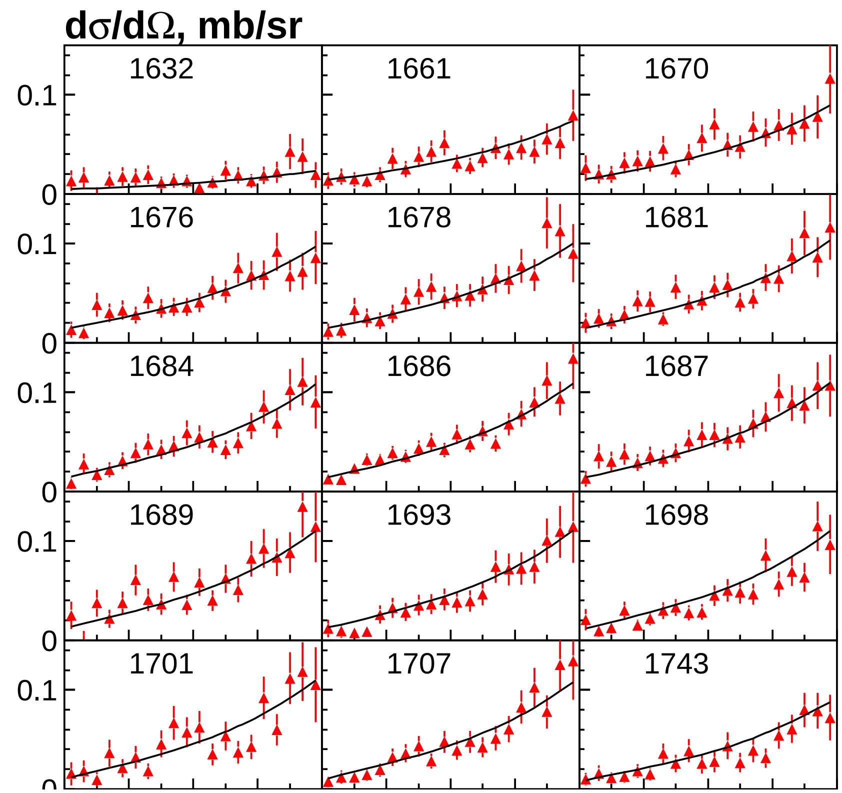

The fit of the the $\pi^- p \to K\Lambda$ reaction

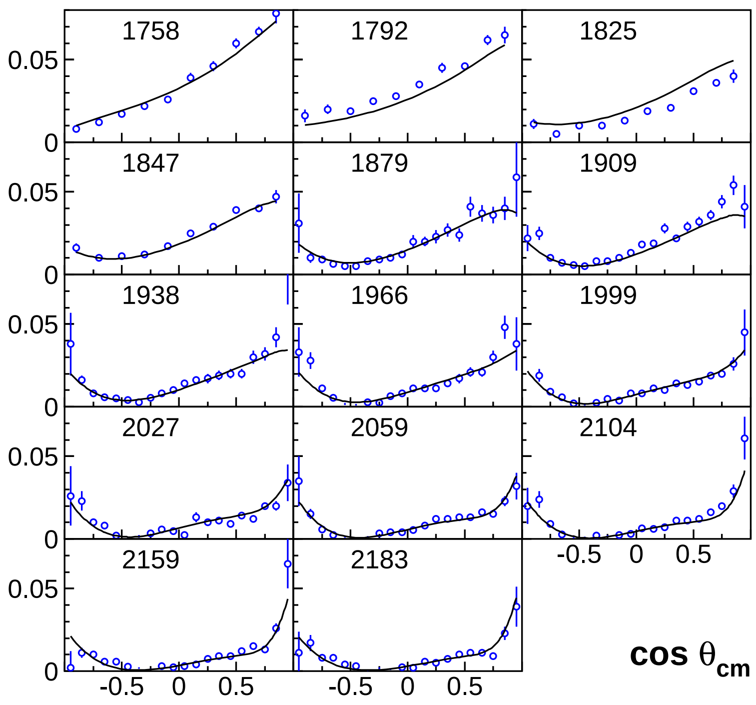

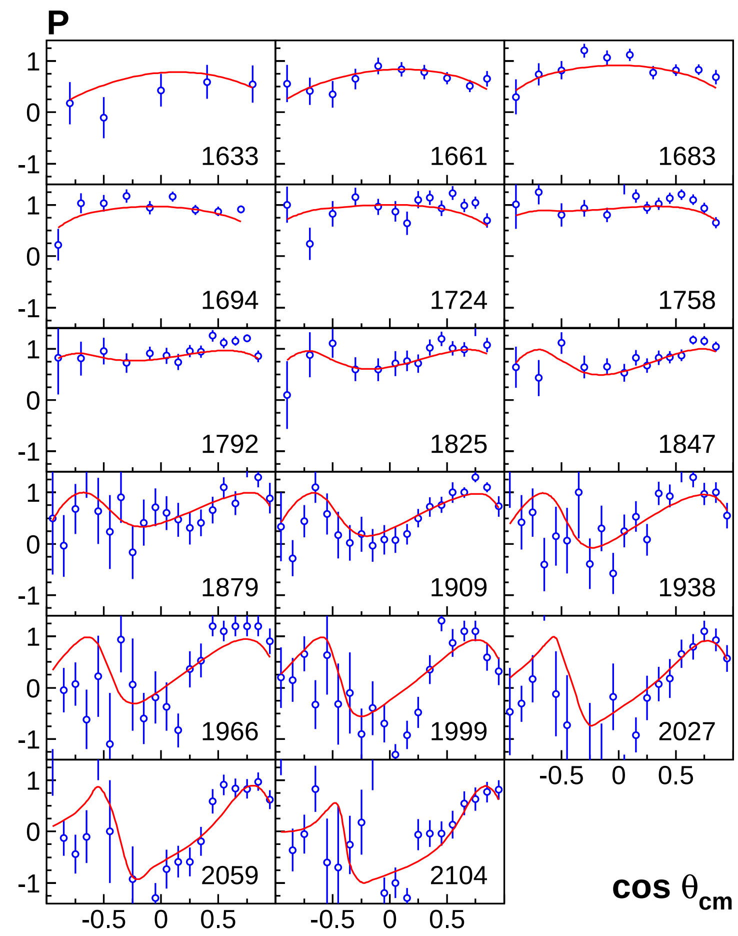

The fit of the the $\pi^+ p \to K^+ \Sigma^+$ reaction

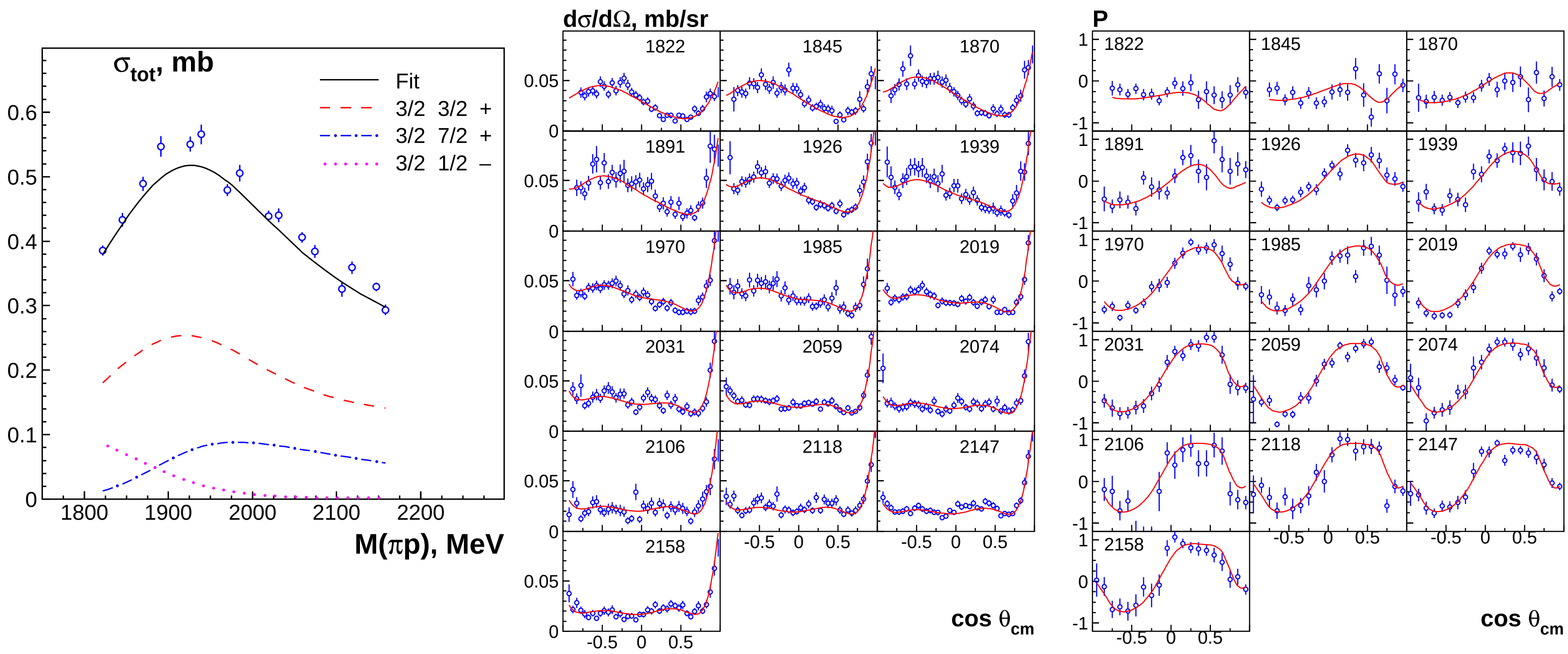

The fit of the the $\pi^- p \to K^0\Sigma^0$ reaction

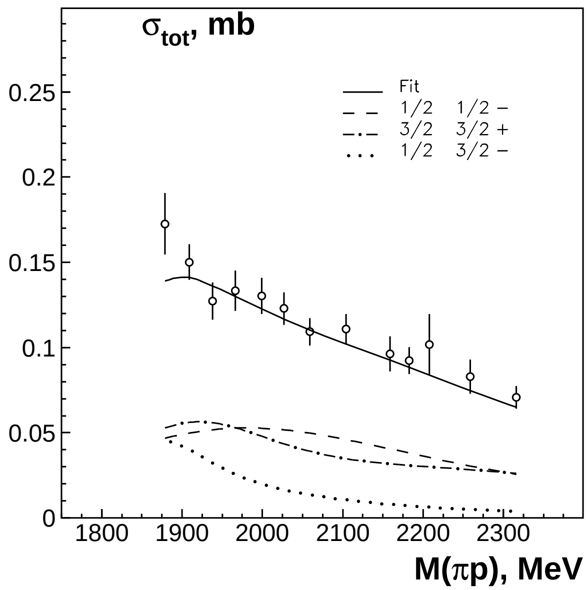

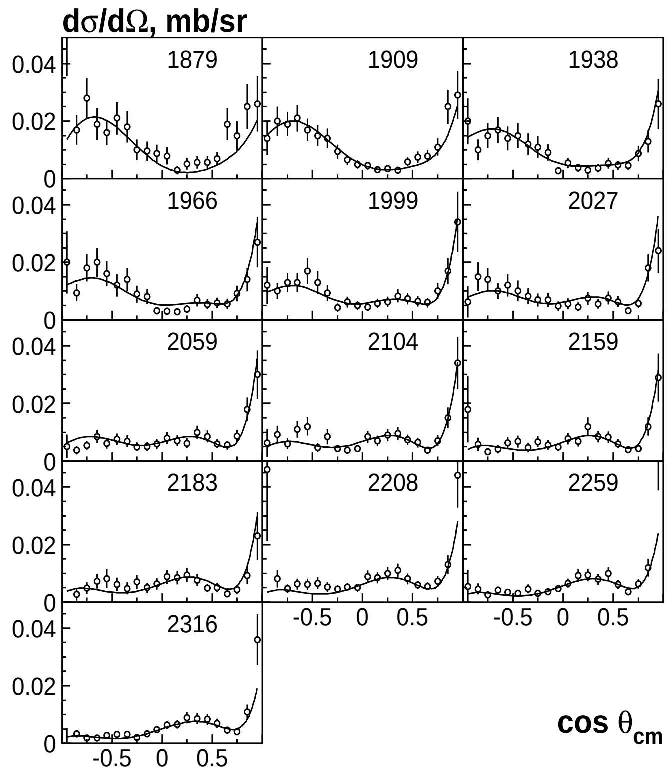

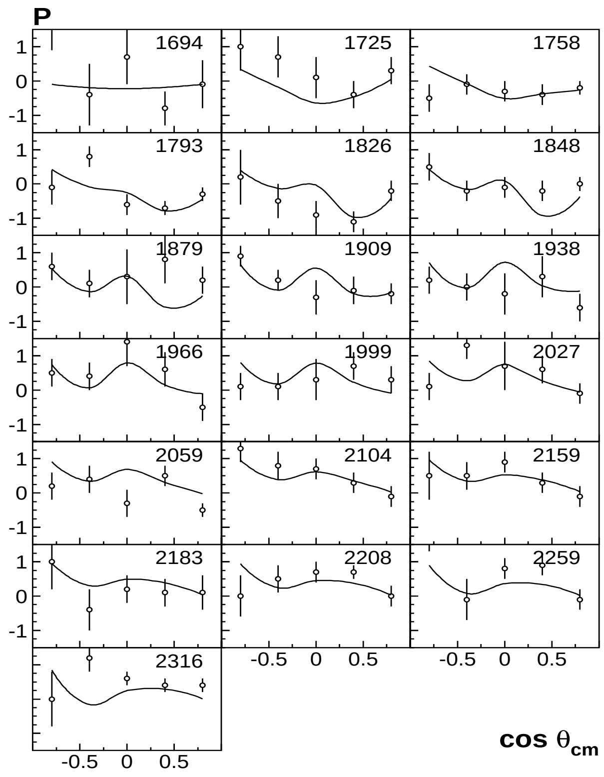

The fit of the $\pi^- p \to \eta n$ reaction

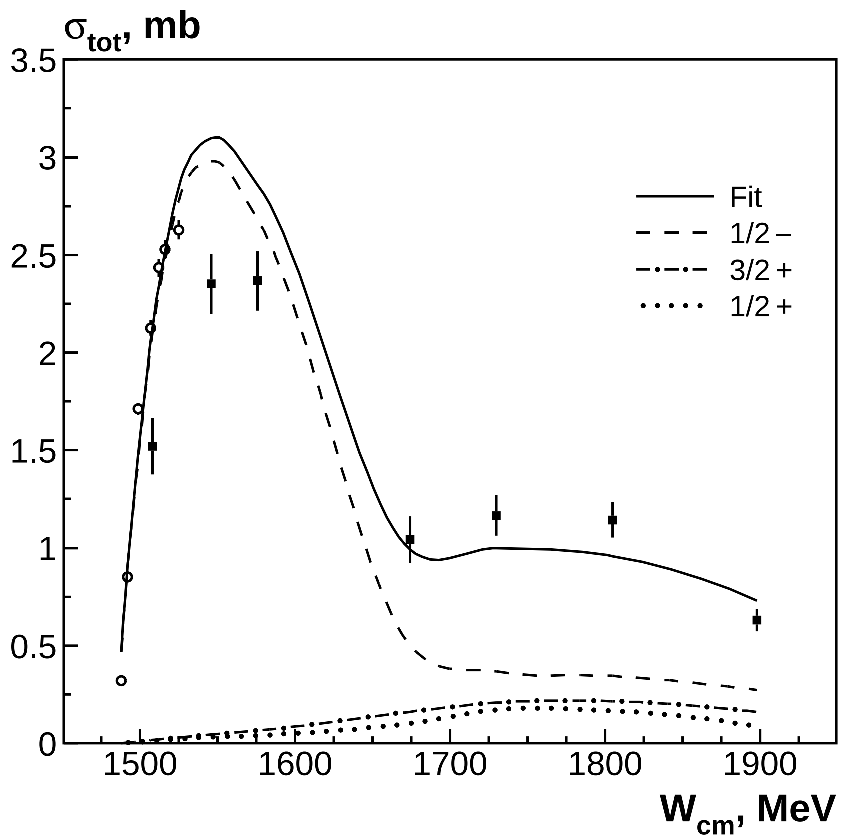

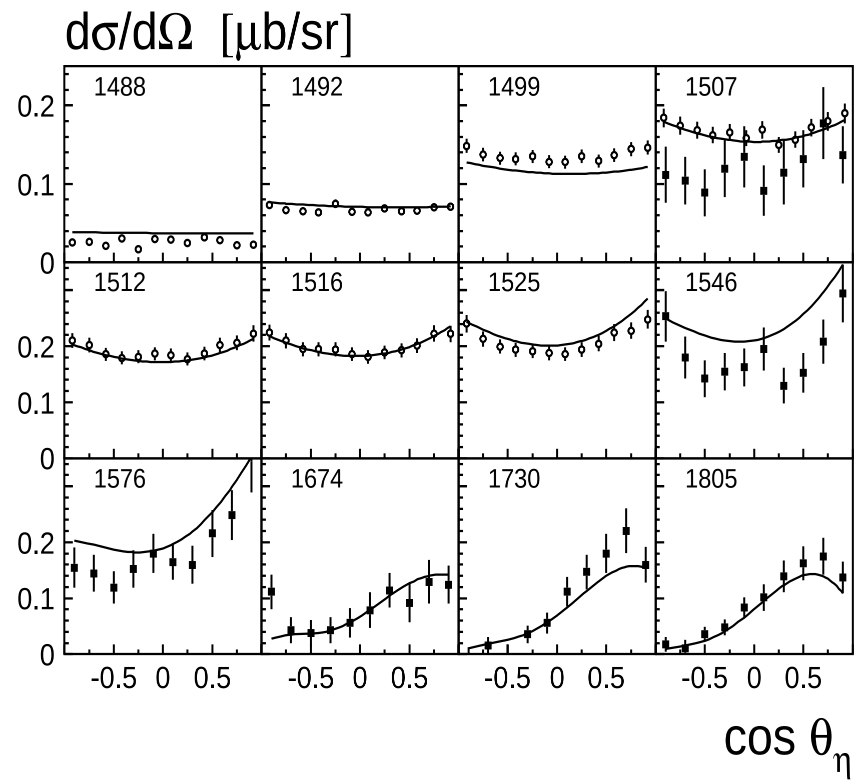

$\pi^- p \to n\pi^0\pi^0$ (Crystal Ball) total cross section

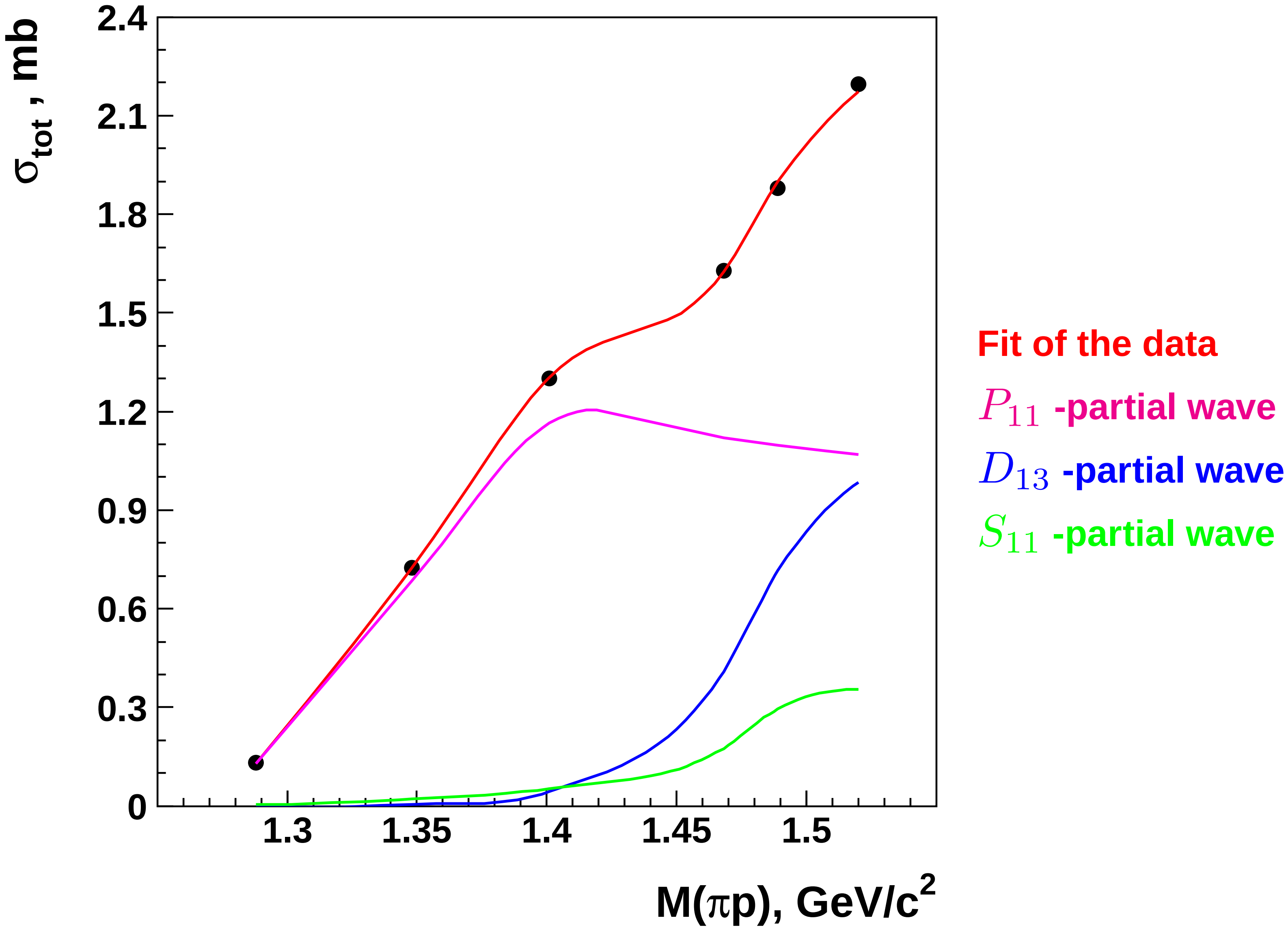

$\pi^- p \to n\pi^0\pi^0$ (Crystal Ball)

Differential cross sections for 472 and 665 MeV/c data.

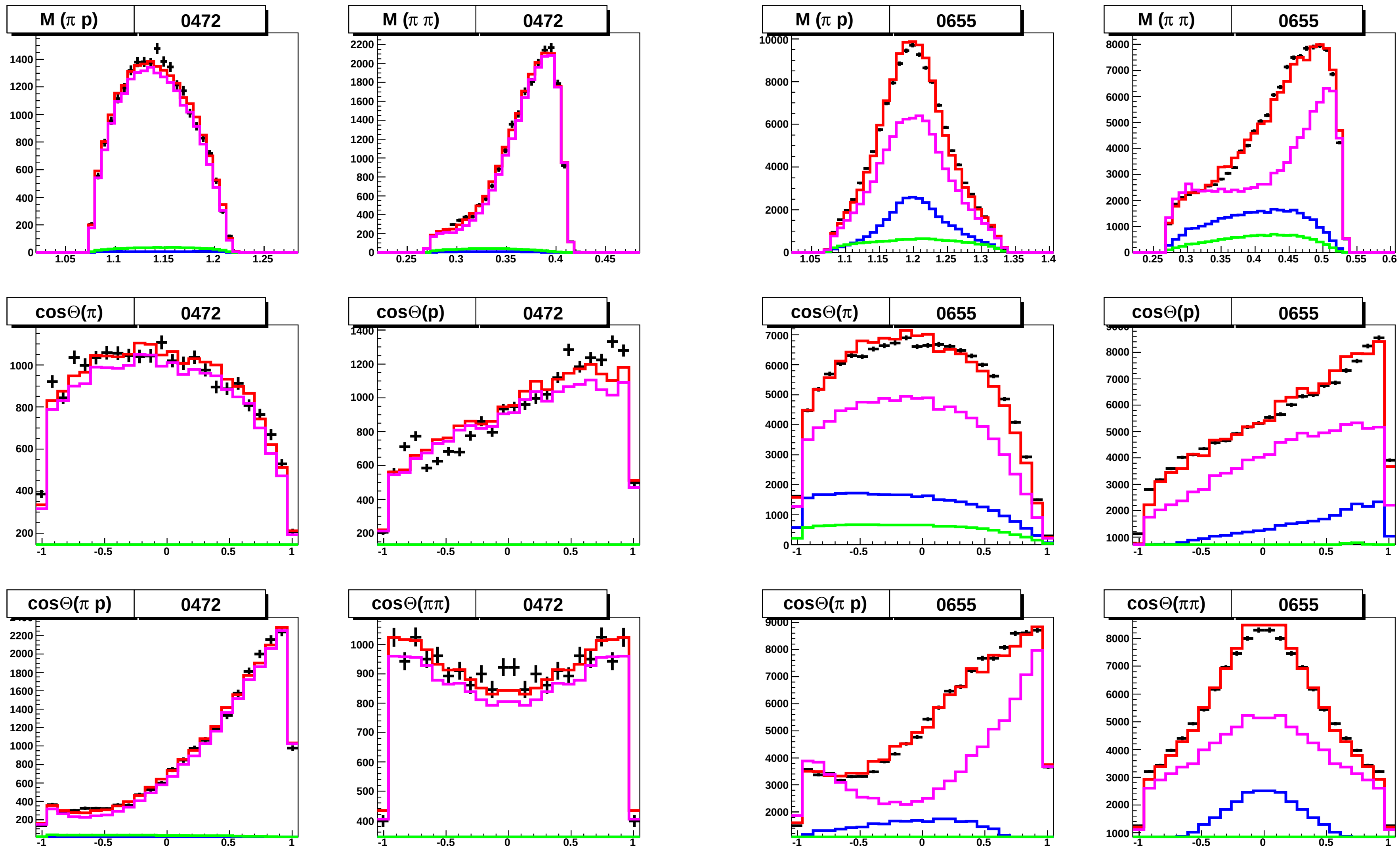

The description of all fitted single meson photoproduction observables as well as multipoles can be downloaded in numerical form or as PDF figures from

PWA.HISKP.UNI-BONN.DE

The $\gamma p \to K\Lambda$ reaction (CLAS 2009)

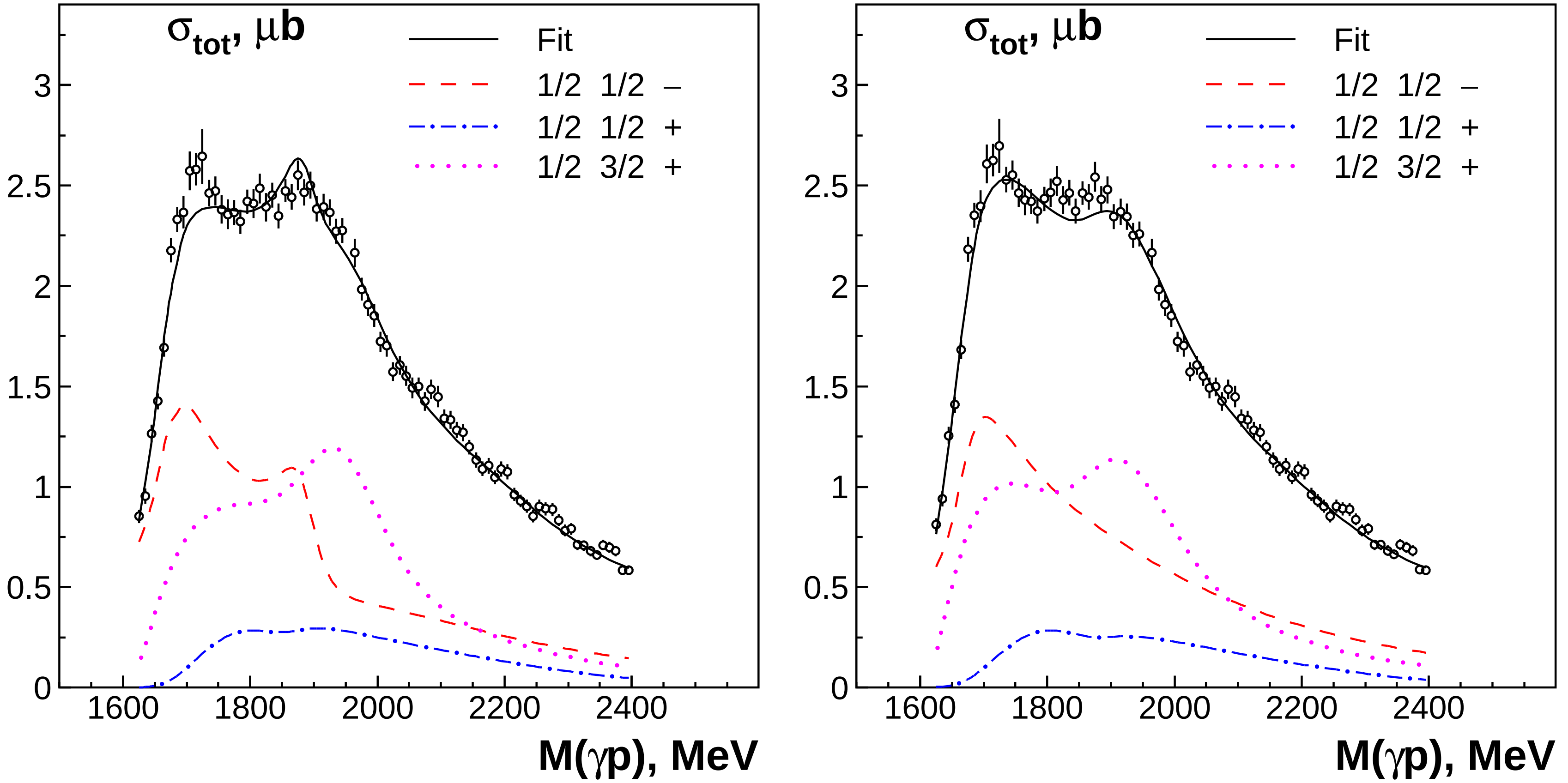

In the first solution the new S_{11} state with mass 1890 ± 10 MeV and width 90 ± 10 MeV is introduced in the fit.

The fit of the $\gamma p \to K\Lambda$ differential cross section

(CLAS 2009)

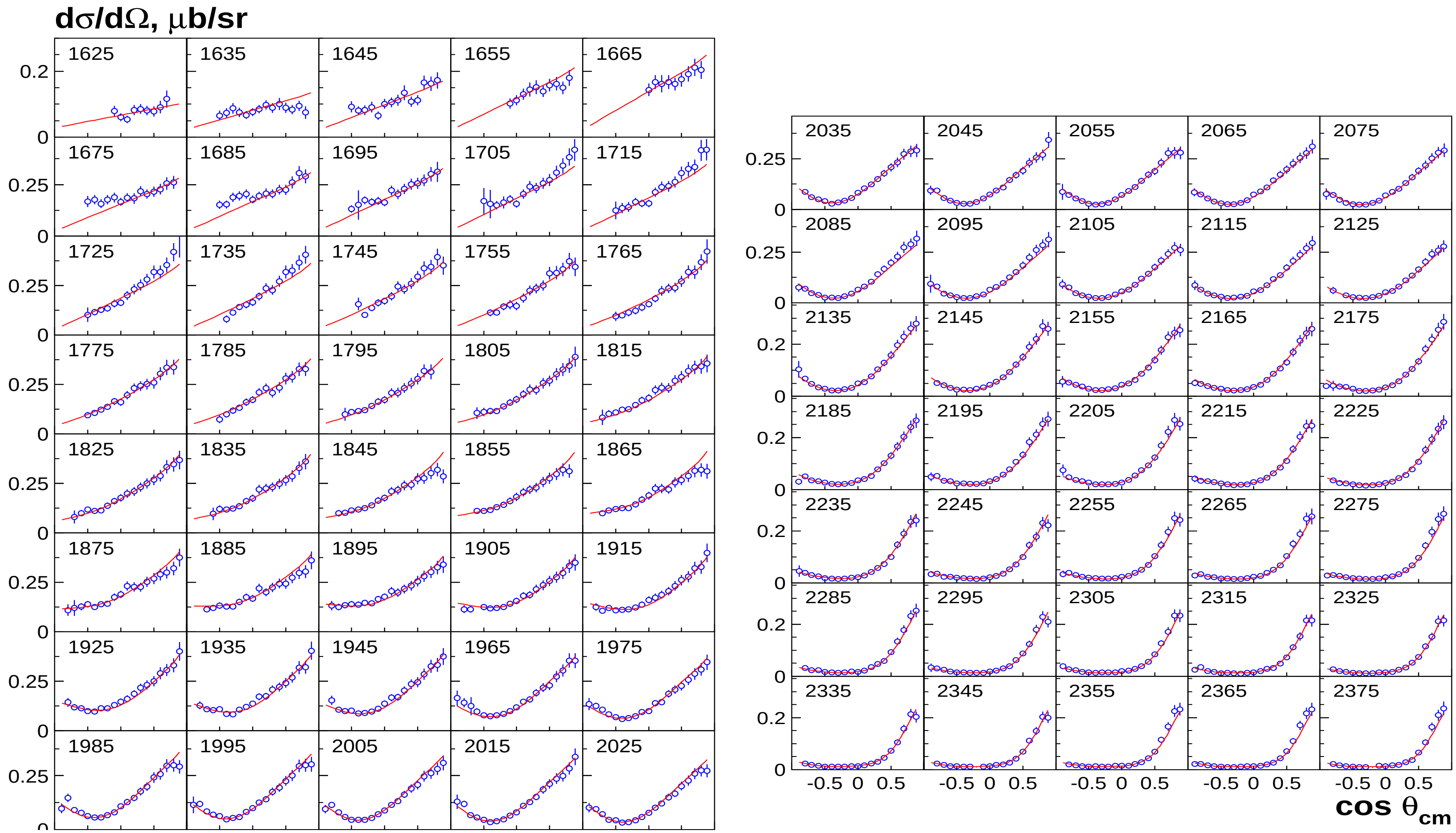

The fit of the $\gamma p \to K\Lambda$ recoil asymmetry

(CLAS 2009)

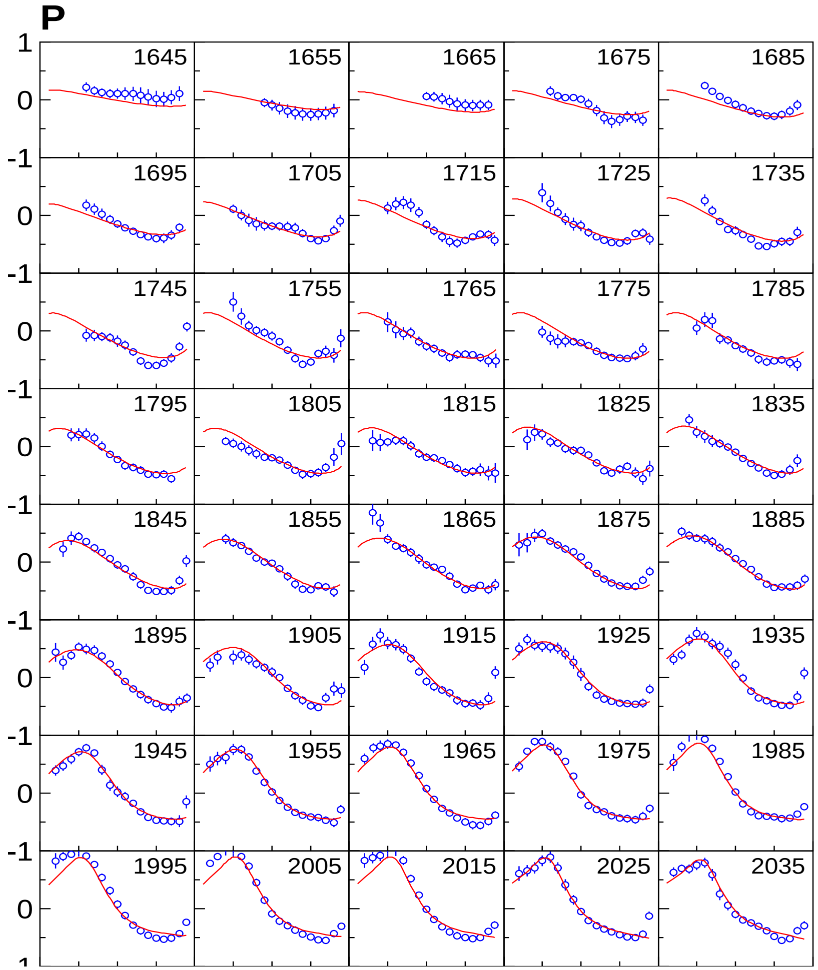

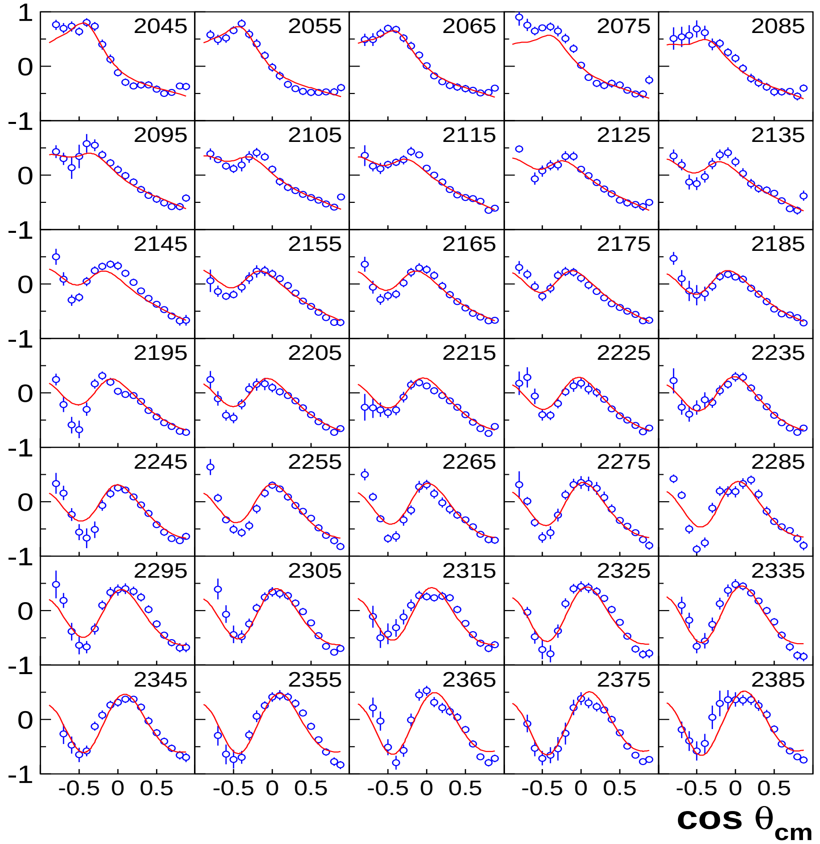

The O_x, O_z and T observables from the $\gamma p \rightarrow K\Lambda$ reaction (GRAAL)

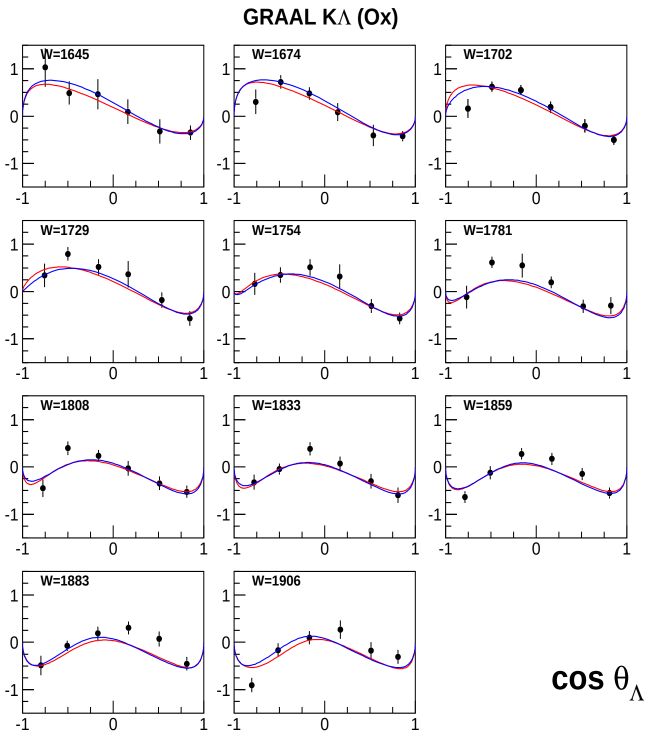

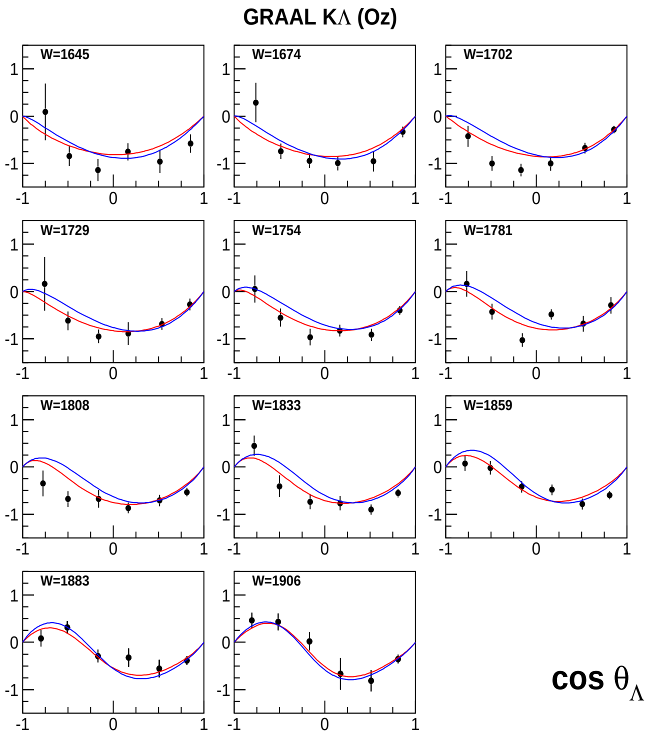

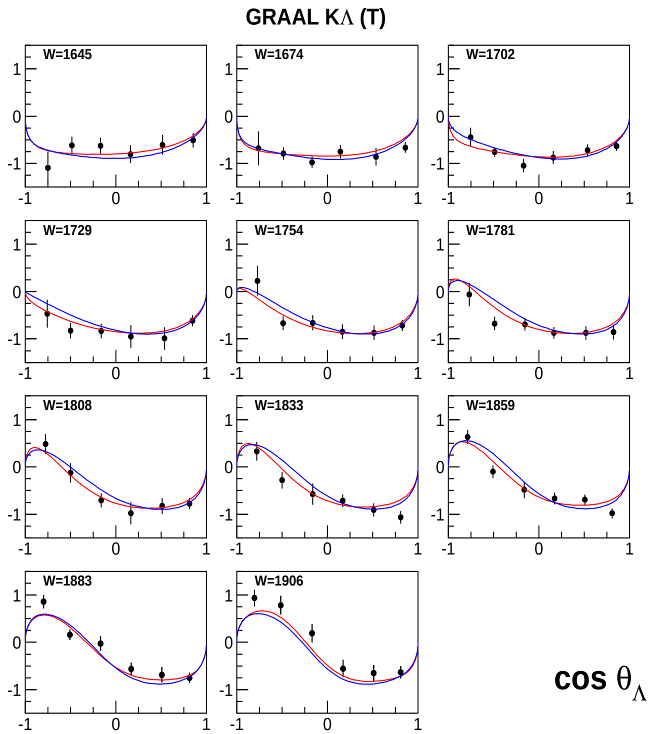

$\gamma p \to p\pi^0\pi^0$ (CB-ELSA) (1.4 GeV)

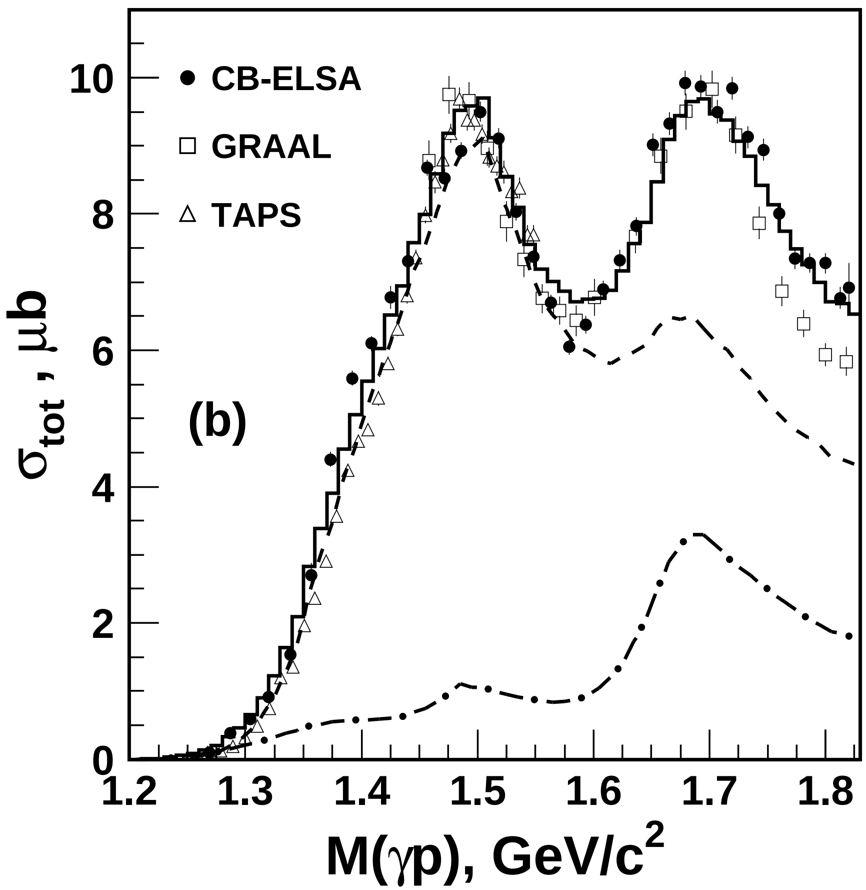

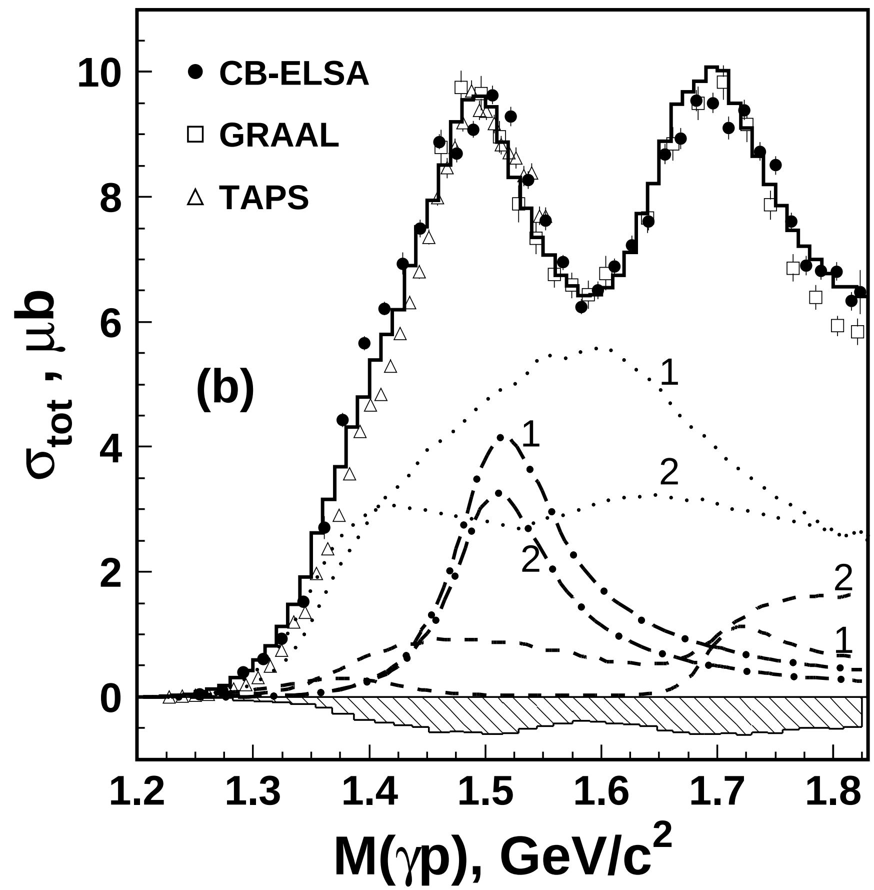

PWA corrected cross section and contributions from $\Delta(1232)\pi$ (dashed) and $N\sigma$ (dashed-dotted) final states.

Contributions from D_{33} (dotted), P_{11} (dashed) and D_{13} (dashed-dotted) partial waves.

$\gamma p \to p\pi^0\pi^0$ (CB-ELSA) (3.2 GeV)

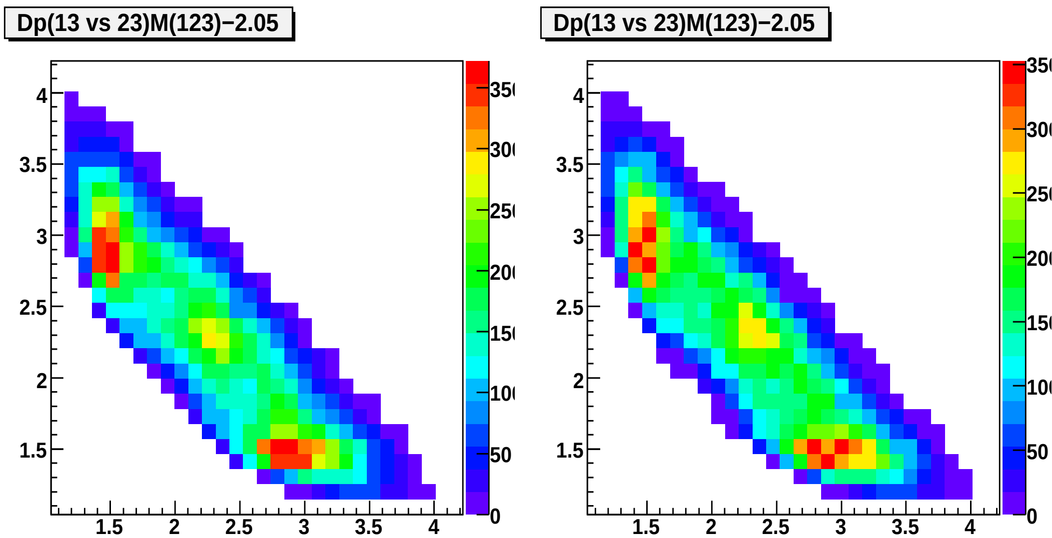

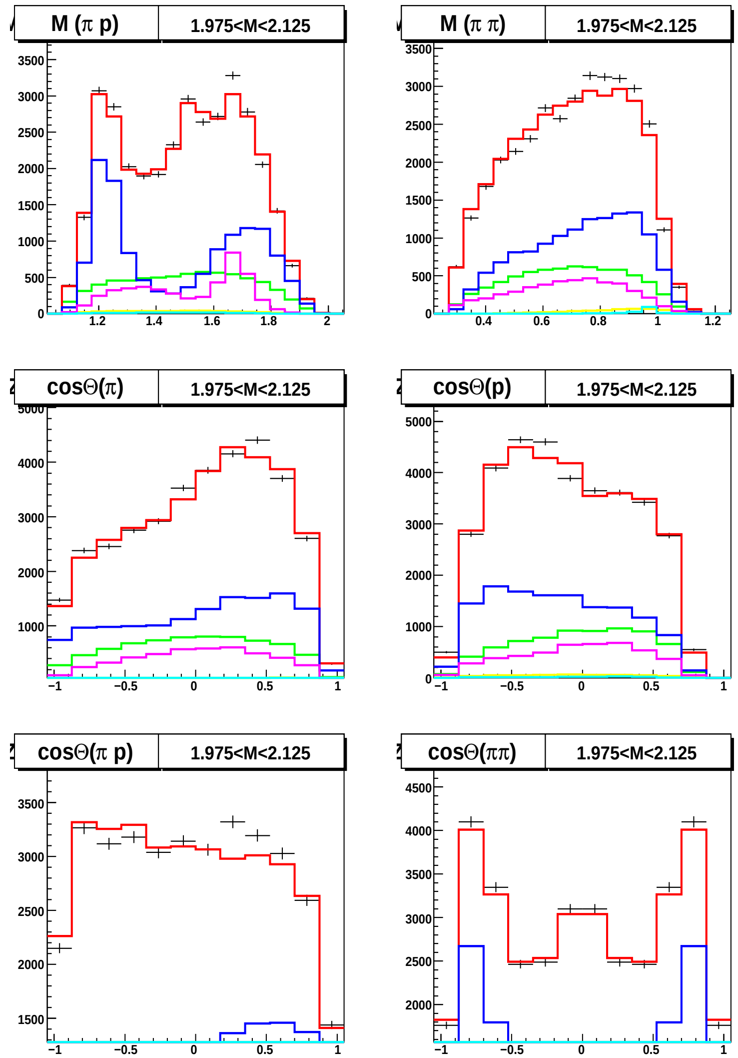

Contributions from $D_{13}(1520)\pi$ and $F_{15}(1650)\pi$

$\gamma p \to p\pi^0\eta$ (CB-ELSA)

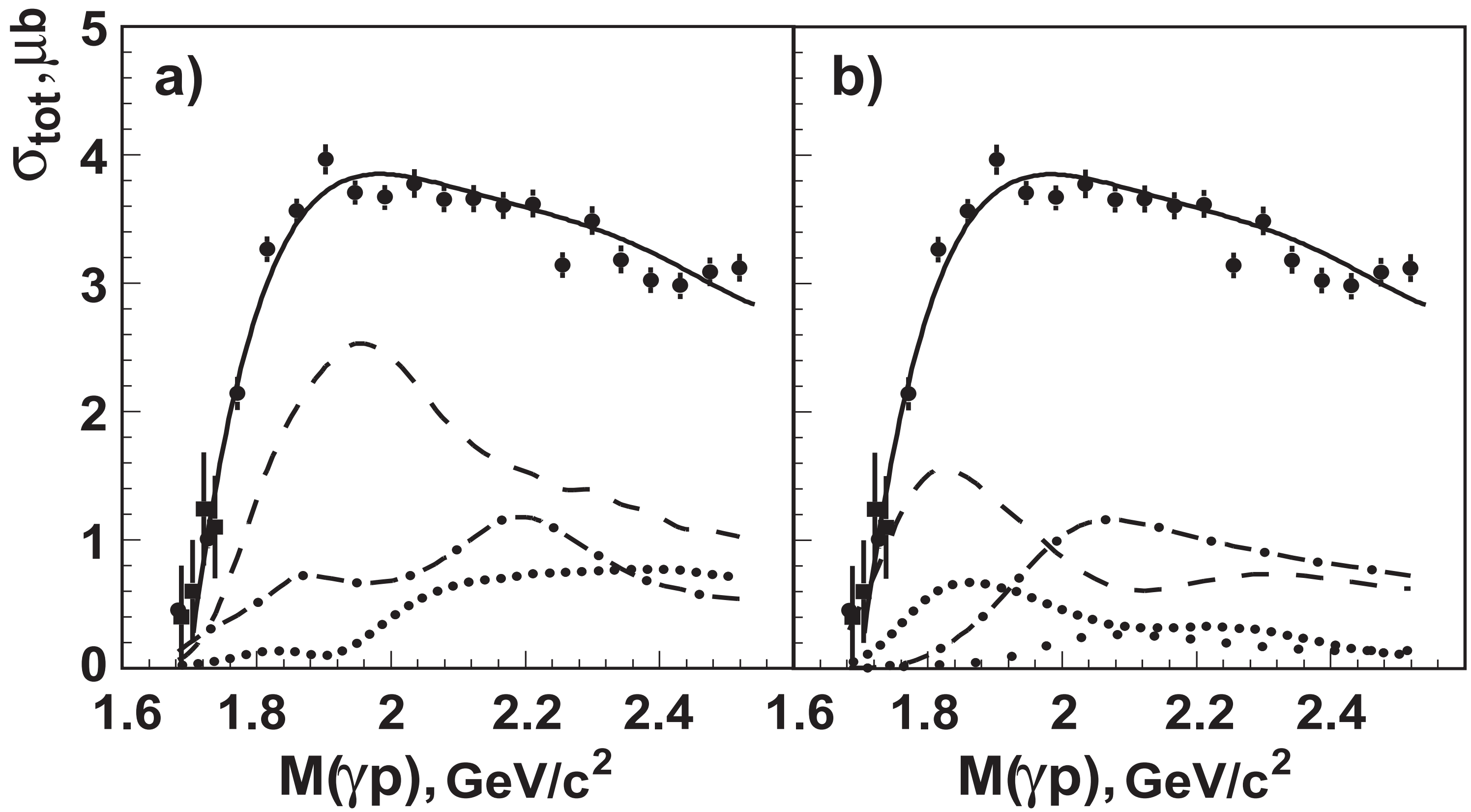

Left panel : contributions from $\Delta(1232)\eta$ (dashed), $S_{11}(1535)\pi$ (dashed-dotted) and $N\,a_0(980)$ final states.

Right panel: D_{33} partial wave (dashed), P_{33} partial wave (dashed-dotted), $D_{33} \to \Delta(1232)\eta$ (dotted) and $D_{33} \to N\,a_0(980)$ (wide dotted).

The $\gamma p \to \pi^0 \eta p$ differential cross section for the total energy region.

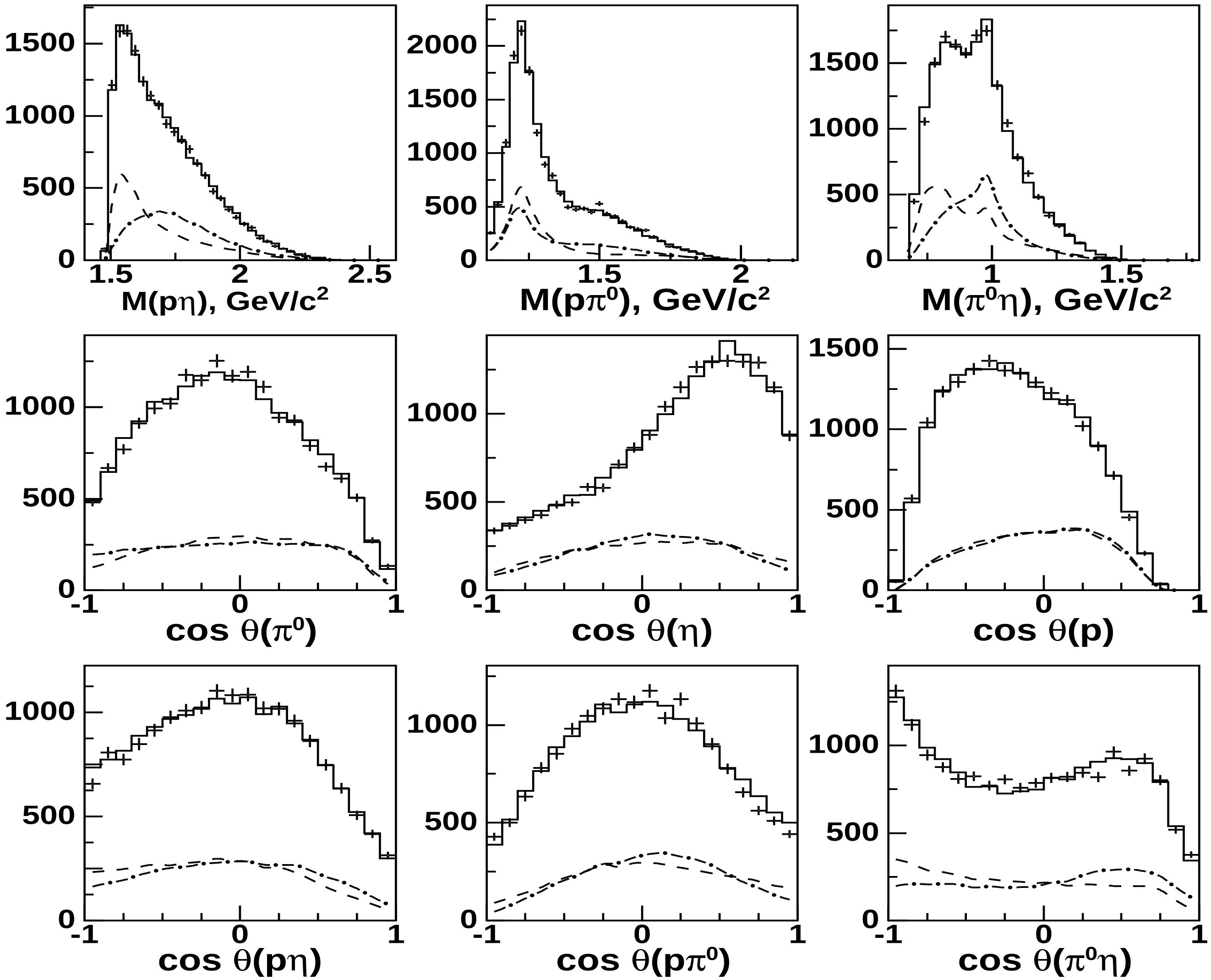

$\gamma p \to p\pi^0\eta$ (CB-ELSA)with linear polarized photon

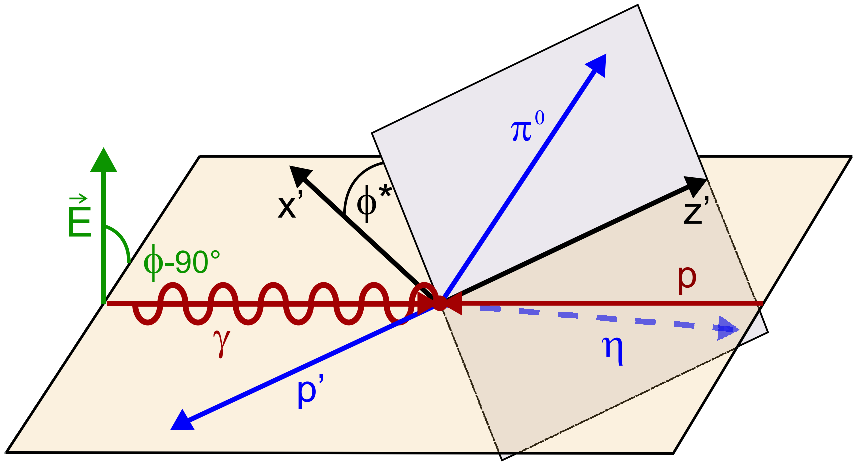

$$\frac{d\sigma}{d\Omega} = \left(\frac{d\sigma}{d\Omega}\right)_0 \{1 + \delta_l [I^s \sin(2\phi) + I^c \cos(2\phi)]\}\,, \qquad (2)$$

$$\Sigma = \int_0^{2\pi} I^c d\phi^*$$

Beam asymmetry from $\gamma p \to p\pi^0\eta$ (CB-ELSA)

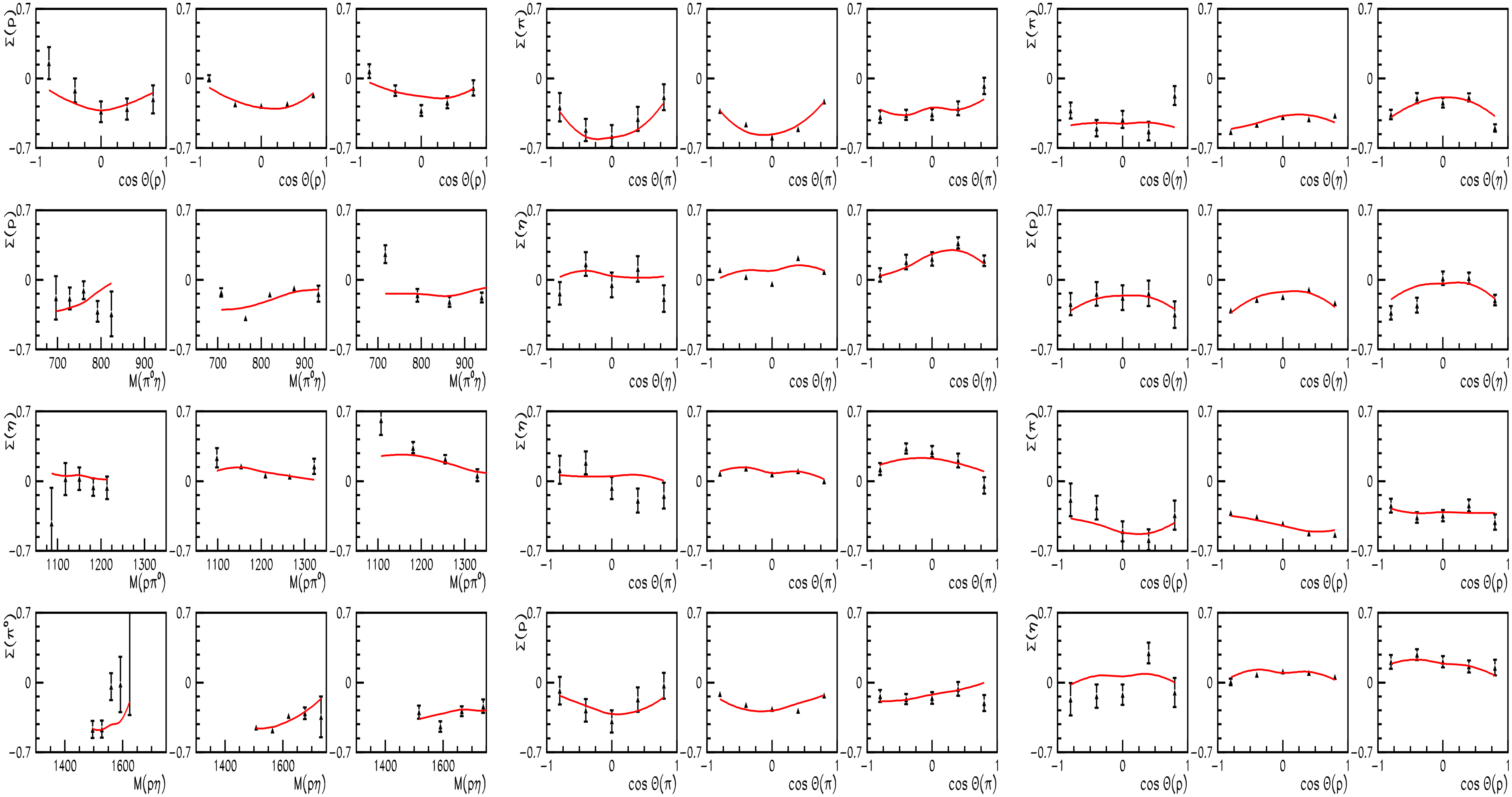

I^c and I^s for $\gamma p \to p\pi^0\eta$ (CB-ELSA)

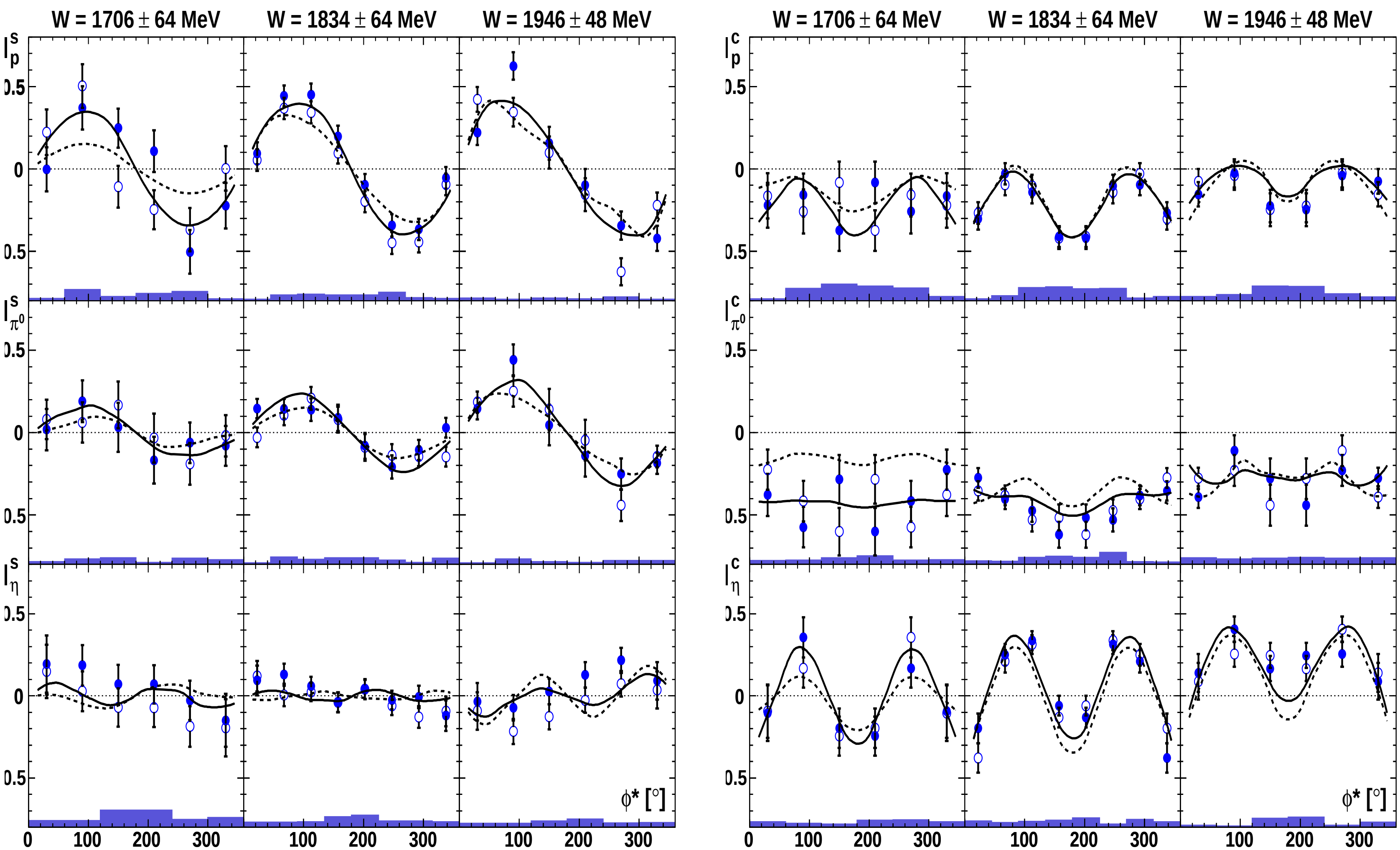

Search for the pole position in the complex plane

One pole many channel K-matrix: relativistic Breit-Wigner amplitude:

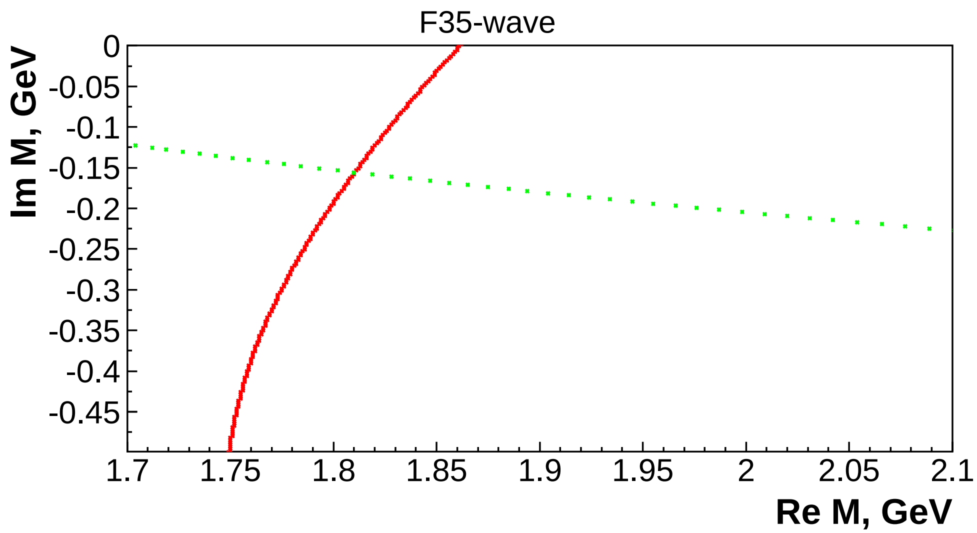

$$Re(M^2 - s - i\sum_j \rho_j(s) g_j^2) = 0$$

$$Im(M^2 - s - i\sum_j \rho_j(s) g_j^2) = 0$$

T-matrix poles: $Re = 1815$ **MeV,** $2\ Im = 310$ **MeV;**

$M_{BW} = 1870$ **MeV,** $\Gamma_{BW} = 345$ **MeV**

And pole residues are complex numbers:

$$\frac{1}{2\pi i}\oint ds A_{ii}(s) = \frac{g_i^2}{1 + i\sum_\alpha g_\alpha^2 \rho'_\alpha(s)}$$

P_{33} wave (3 pole 6 channel K-matrix)

$$D = det(I - i\rho K)\prod_i (M_i^2 - s) \qquad 1\mathrm{-pole}: D = M^2 - s - i\sum_j \rho_j(s) g_j^2$$

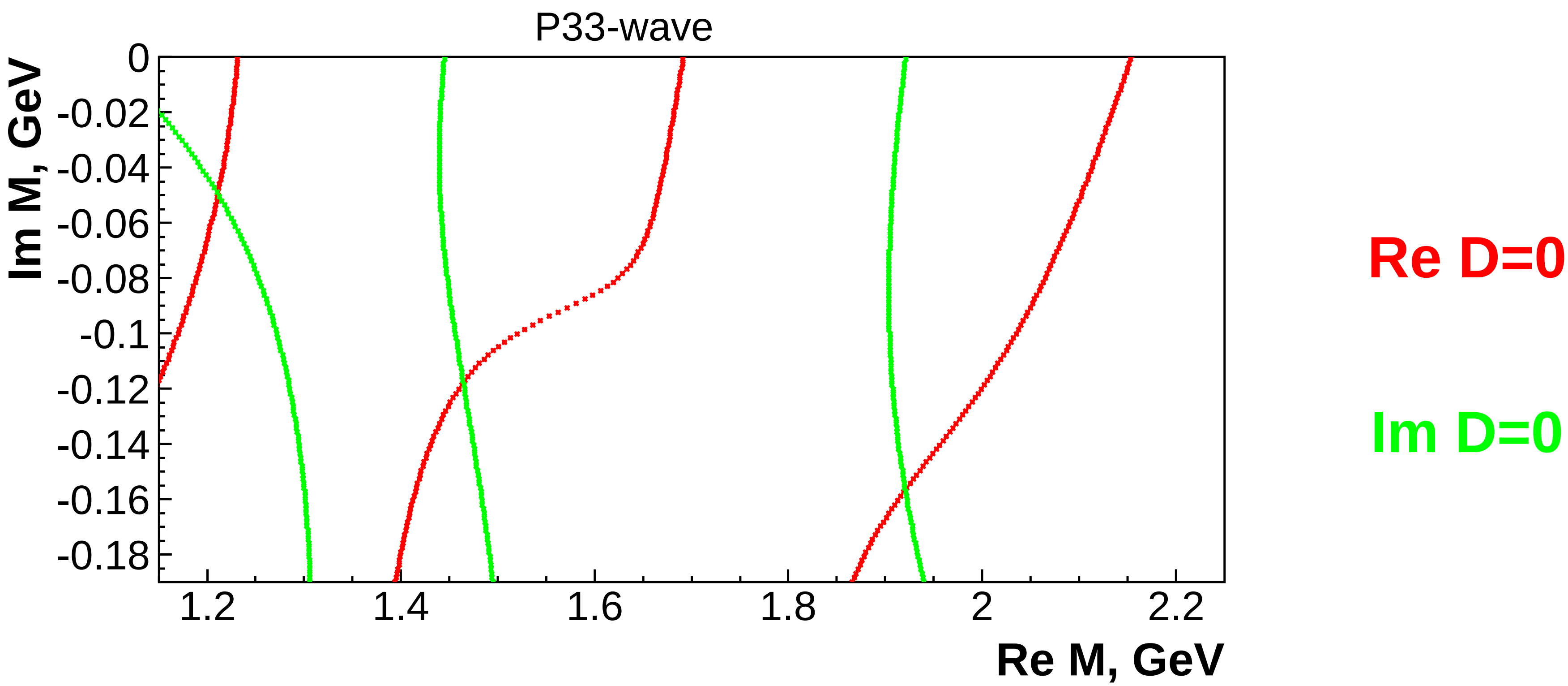

T-matrix poles: $M = 1210 - i50$ **MeV;**

$M = 1485 - i120$ **MeV**

$M = 1920 - i160$ **MeV**

D_{13} wave (3 pole 6 channel K-matrix)

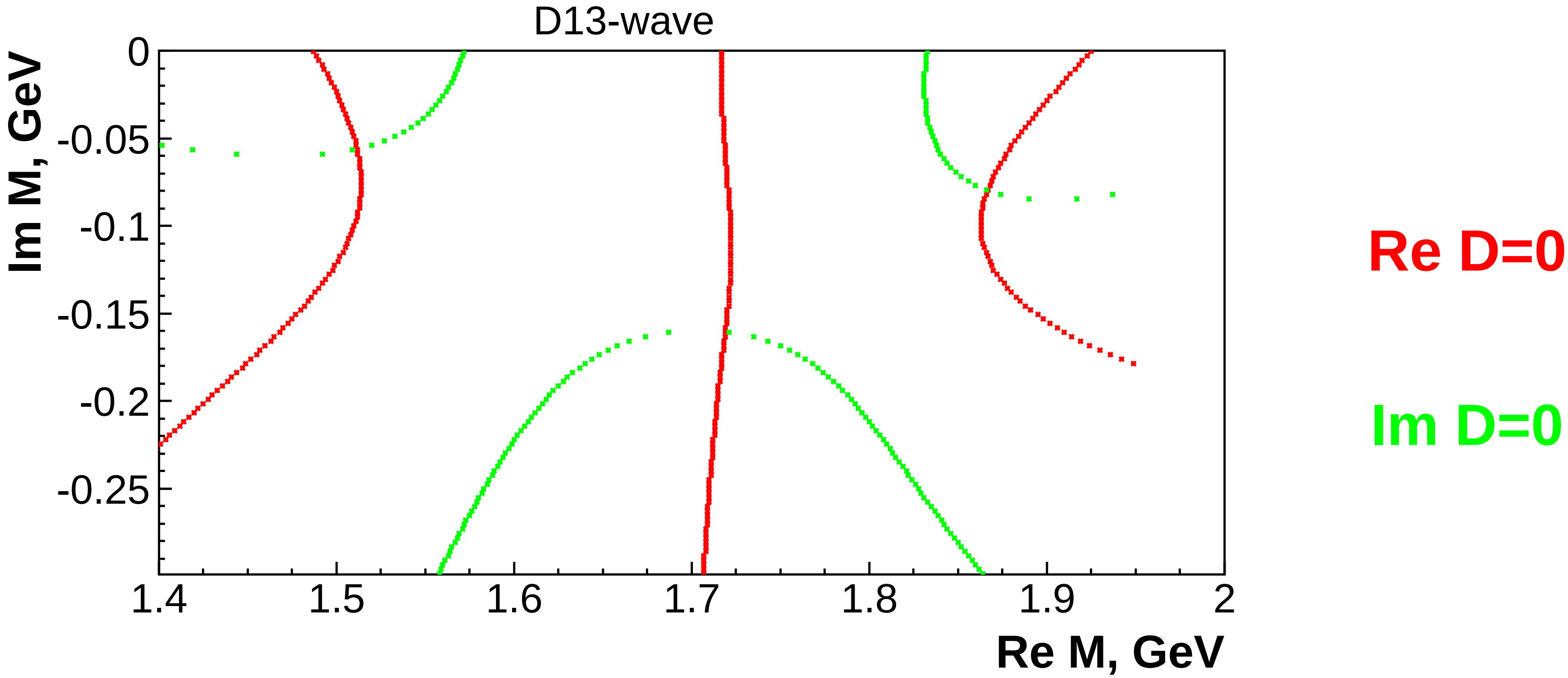

T-matrix poles: $M = 1512 - i55$ **MeV;**

$M = 1720 - i170$ **MeV**

$M = 1860 - i75$ **MeV**

P_{11} wave: 3 pole 6 channel K-matrix (πN, ηN, $K\Lambda$, $K\Sigma$, $\pi\Delta(1232)$, $N\sigma$)

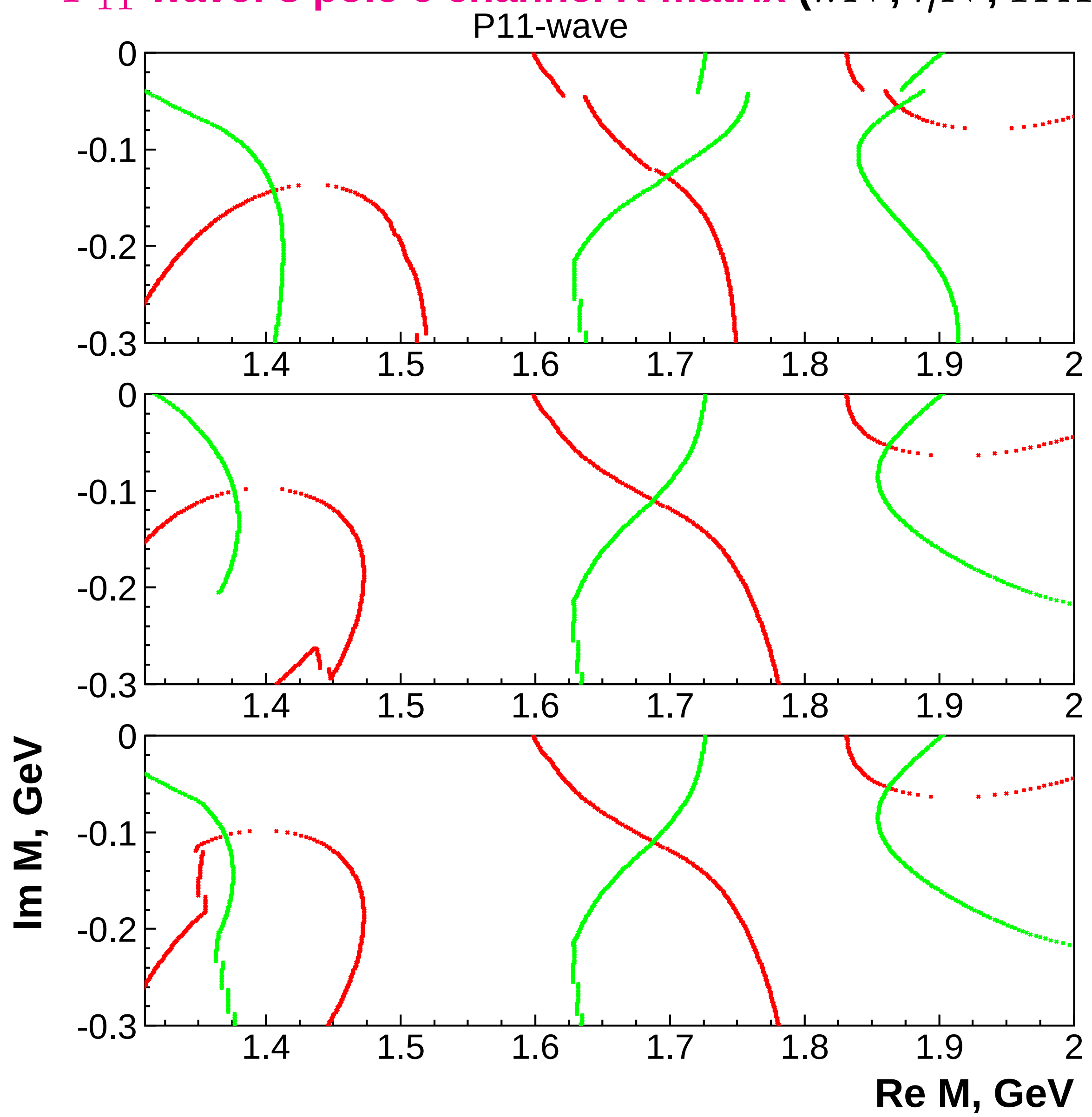

Re D=0

Im D=0

T-matrix poles:

$M = 1370 - i80$ **MeV;**

$M = 1695 - i105$ **MeV**

$M = 1860 - i60$ **MeV**

S_{11}: 2-pole 5-channel K-matrix (πN, ηN, $K\Lambda$, $K\Sigma$ and $\pi\Delta(1232)$)

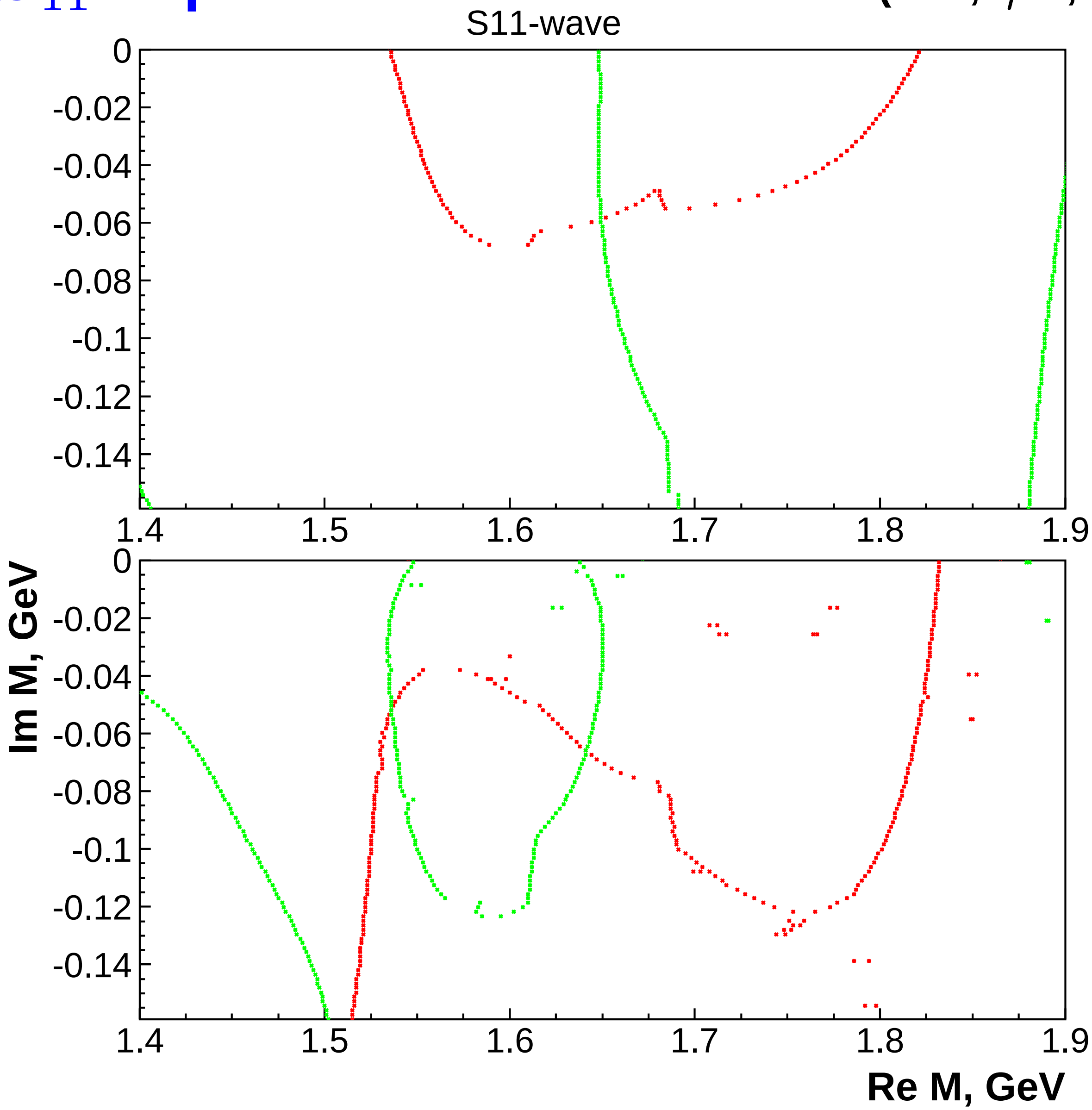

Re D=0

Im D=0

I sheet: closest to the physical region above ηN threshold.

$M = 1650 - i60$ **MeV;**

II sheet: closest to the physical region below ηN threshold.

$M = 1525 - i100$ **MeV**

Calculation of the residues

For any function of complex variables $F(s)$:

$$\oint dsF(s) = \sum_{\alpha} 2\pi i \; Res_{\alpha}$$

The result does not depend on the form of the counter.

Full factorization of the amplitude at the pole position:

$$\oint dsA_{ij}(s) = 2\pi i \; g_i g_j$$

The residues g_i are complex numbers.

Problem: how to compare our results with other analyses?

For example with Breit-Wigner parameters given in PDG.

We construct the following amplitude:

$$A_{ij}^{BW} = \frac{g_i^{BW} g_j^{BW}}{M_{BW}^2 - s - i\beta \sum_i g_i^2 \rho_i}$$

where M_{BW} and β are fitted to reconstruct pole position and g_i^{BW} to reconstruct residues in the pole.

As a cross-check: the procedure works very well for the relativistic Breit-Wigner amplitude

$$(g_i^{BW})^2 \sim \beta g_i^2$$

and width can be estimated as:

$$M_{BW} \Gamma_{tot}^{BW} = Im(i\beta \sum_i g_i^2 \rho_i)$$

However in the case of fast increasing phase volumes the M_{BW} and Γ^{BW}_{tot} also can be hardly compared with PDG data.

It is better to compare the maximum in πN elastic amplitude squared and width at half height.

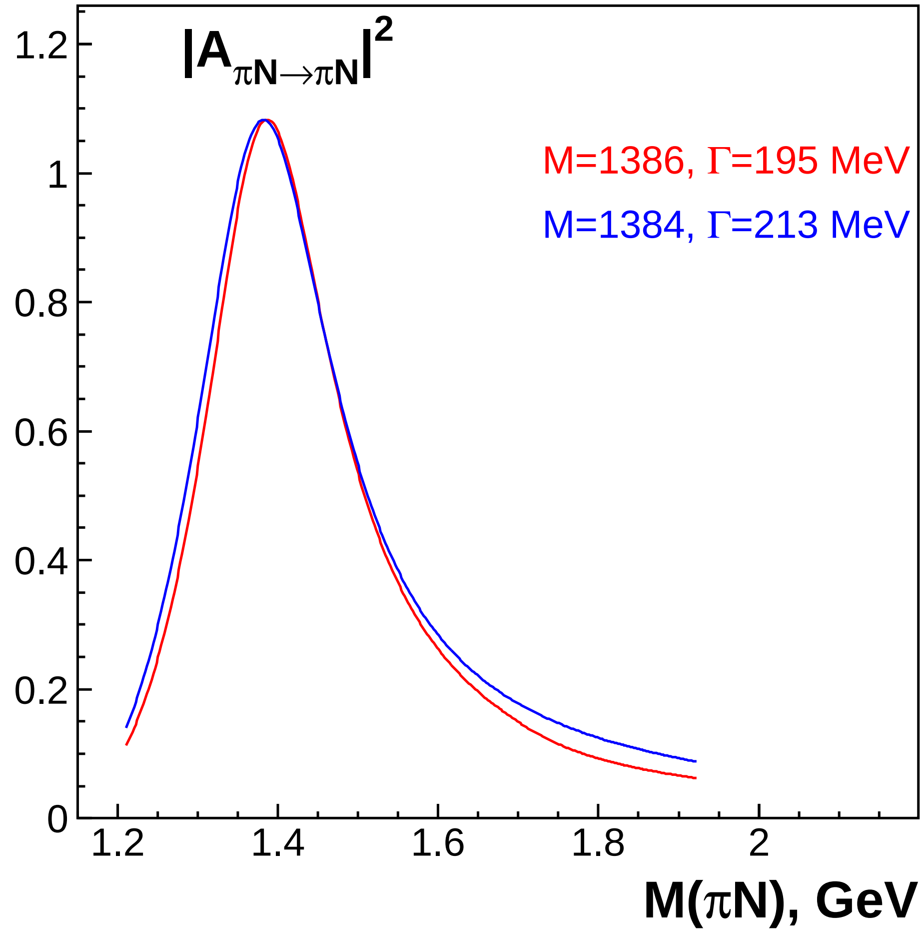

M_{BW}=**1410 MeV** Γ^{BW}_{tot}=**350 MeV**

M_{BW}=**1470 MeV** Γ^{BW}_{tot}=**550 MeV**

P_{13}: 3-pole 8-channel K-matrix

(πN, ηN, $K\Lambda$, $K\Sigma$, $\pi\Delta(1232)$(P,F),$N\sigma$, $D_{13}(1520)\pi$)

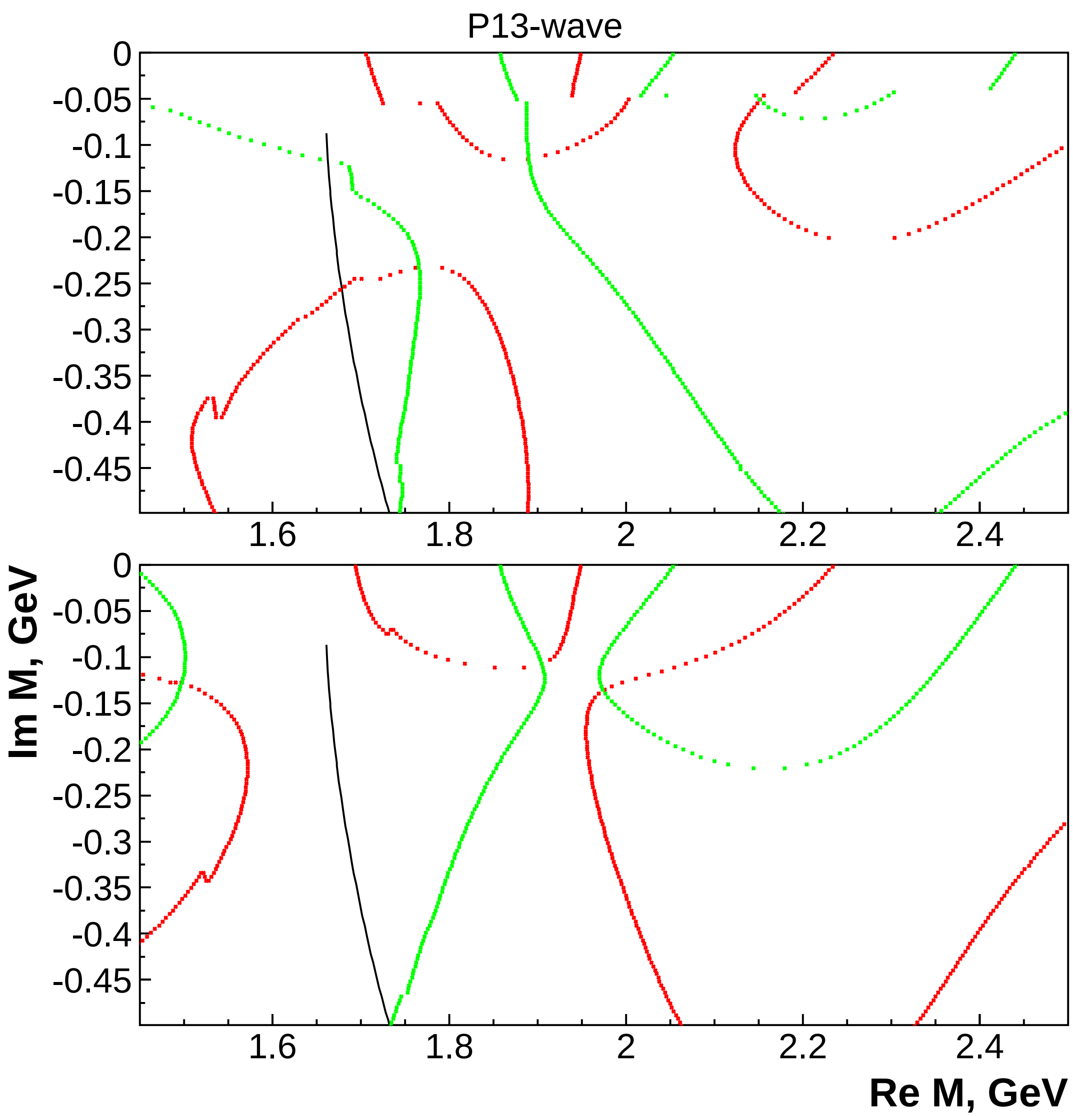

Re D=0 **Im D=0**

I sheet: closest to the physical region below $D_{13}(1520)\pi$ threshold.

$M = 1730 - i230$ **MeV;**

II sheet: closest to the physical region above $D_{13}(1520)\pi$ threshold.

$M = 1500 - i125$ **MeV**

$M = 1900 - i100$ **MeV**

$M = 1980 - i140$ **MeV**

The effective mass and width are rather close for both poles BW approximations

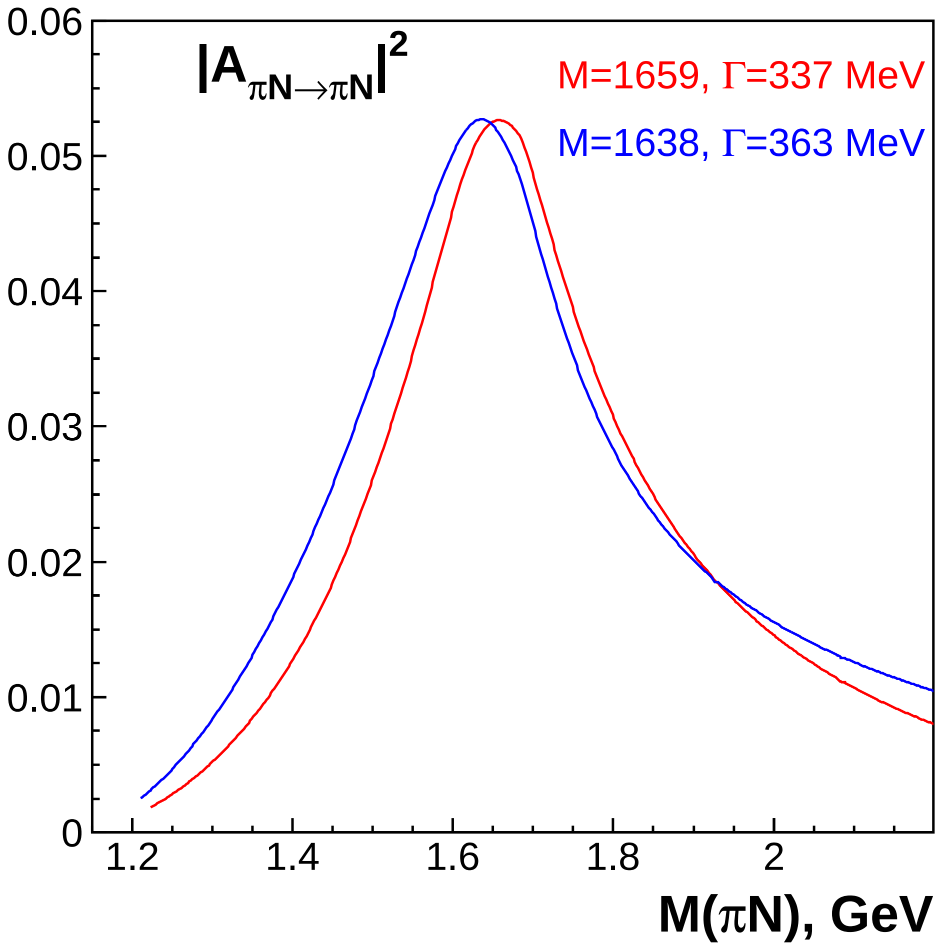

M_{BW}**=1800 MeV** Γ^{BW}_{tot}**=650 MeV**

M_{BW}**=1950 MeV** Γ^{BW}_{tot}**=1500 MeV**

S11-wave transition amplitudes

$\pi N \to \pi N$

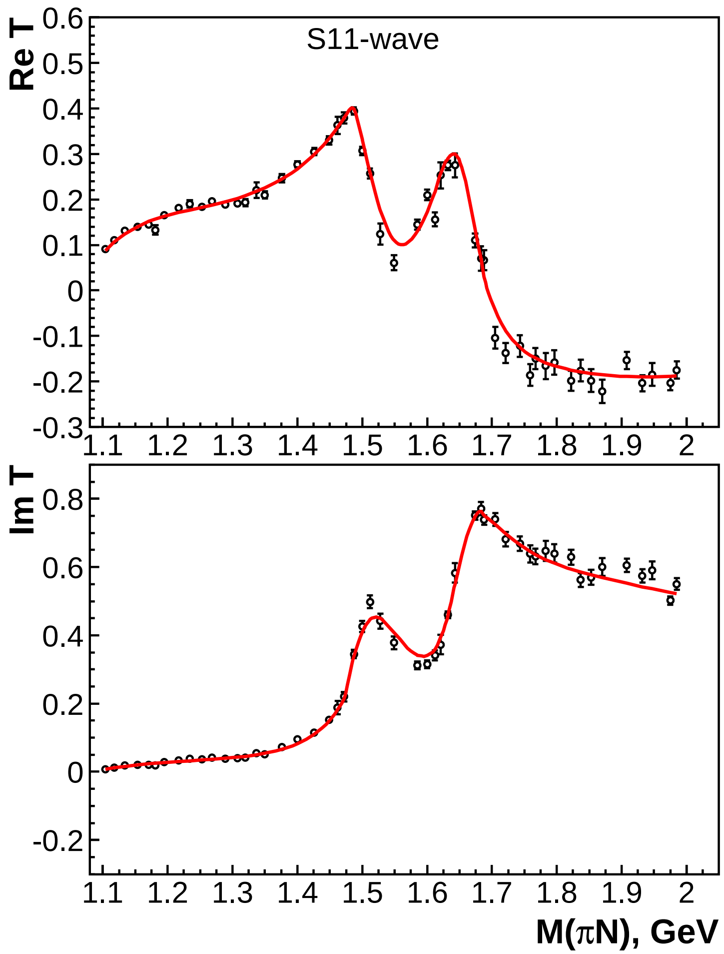

$\pi N \to \pi \Delta(1232)$

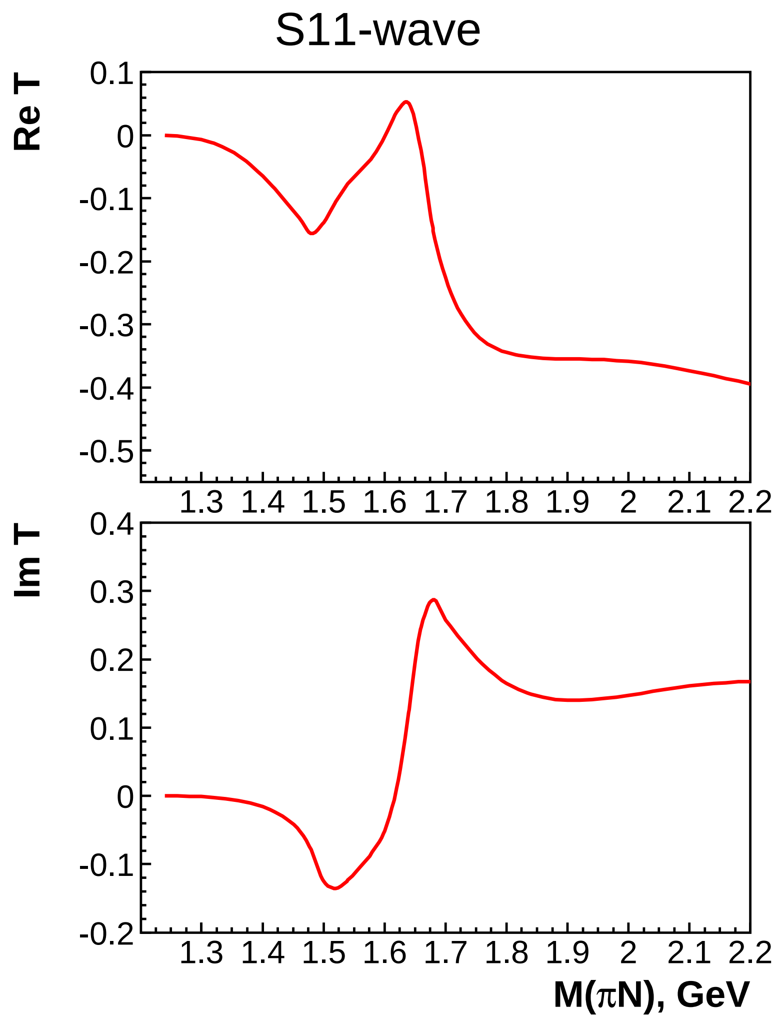

S11-wave transition amplitudes

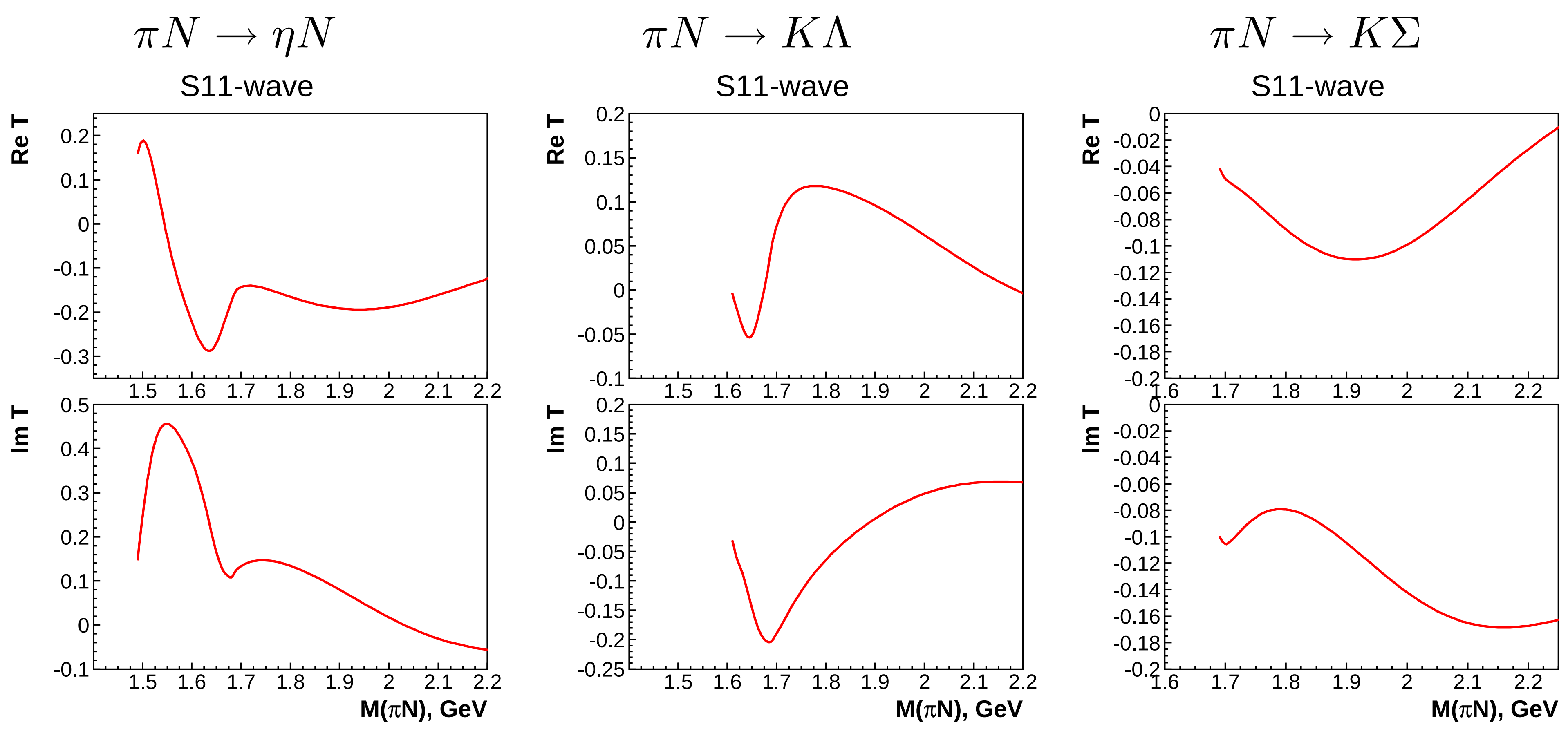

P11-wave transition amplitudes

$\pi N \to \pi N$ $\pi N \to \pi \Delta(1232)$

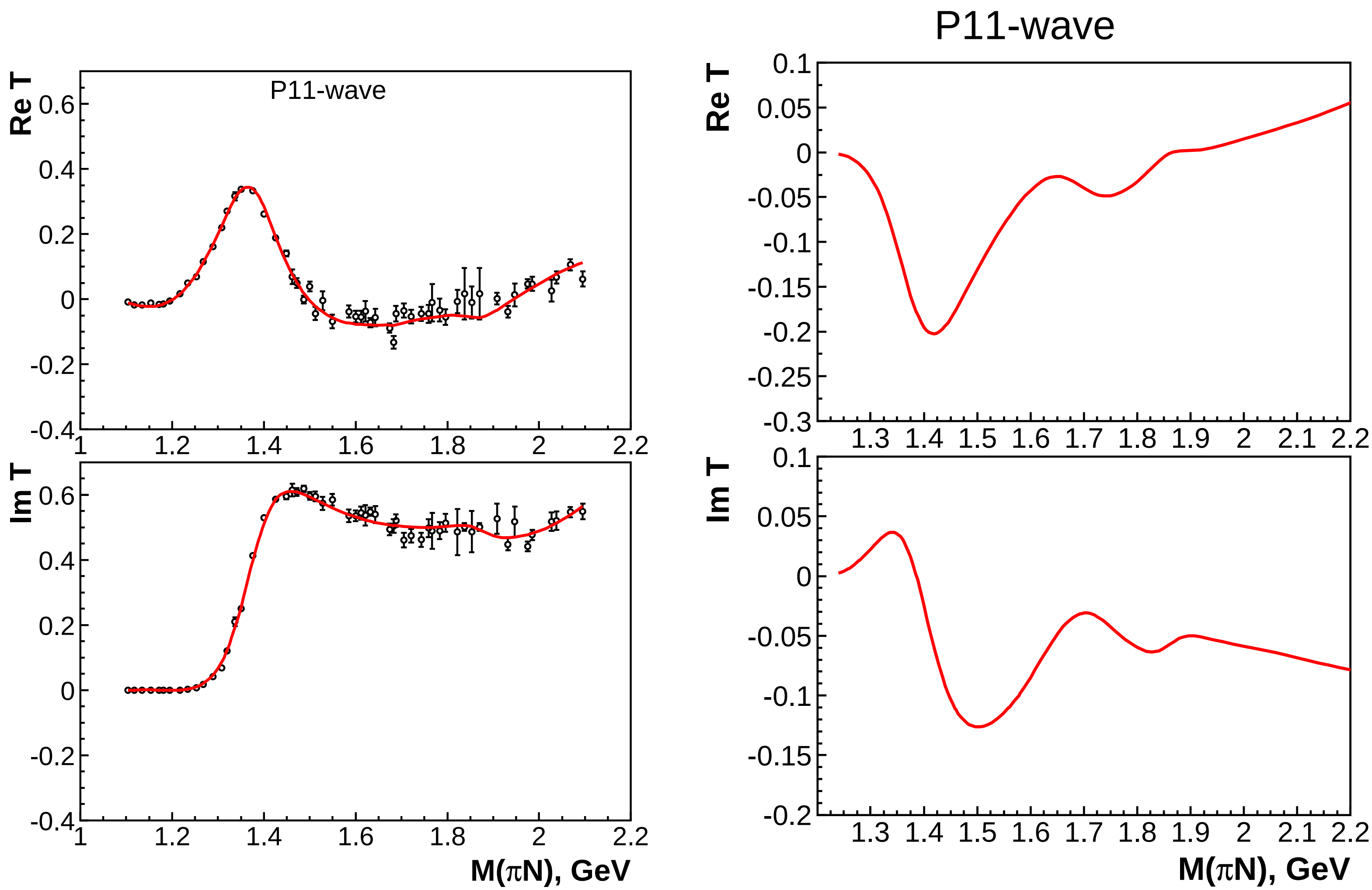

P11-wave transition amplitudes

$\pi N \to \eta N$ $\pi N \to K\Lambda$ $\pi N \to K\Sigma$

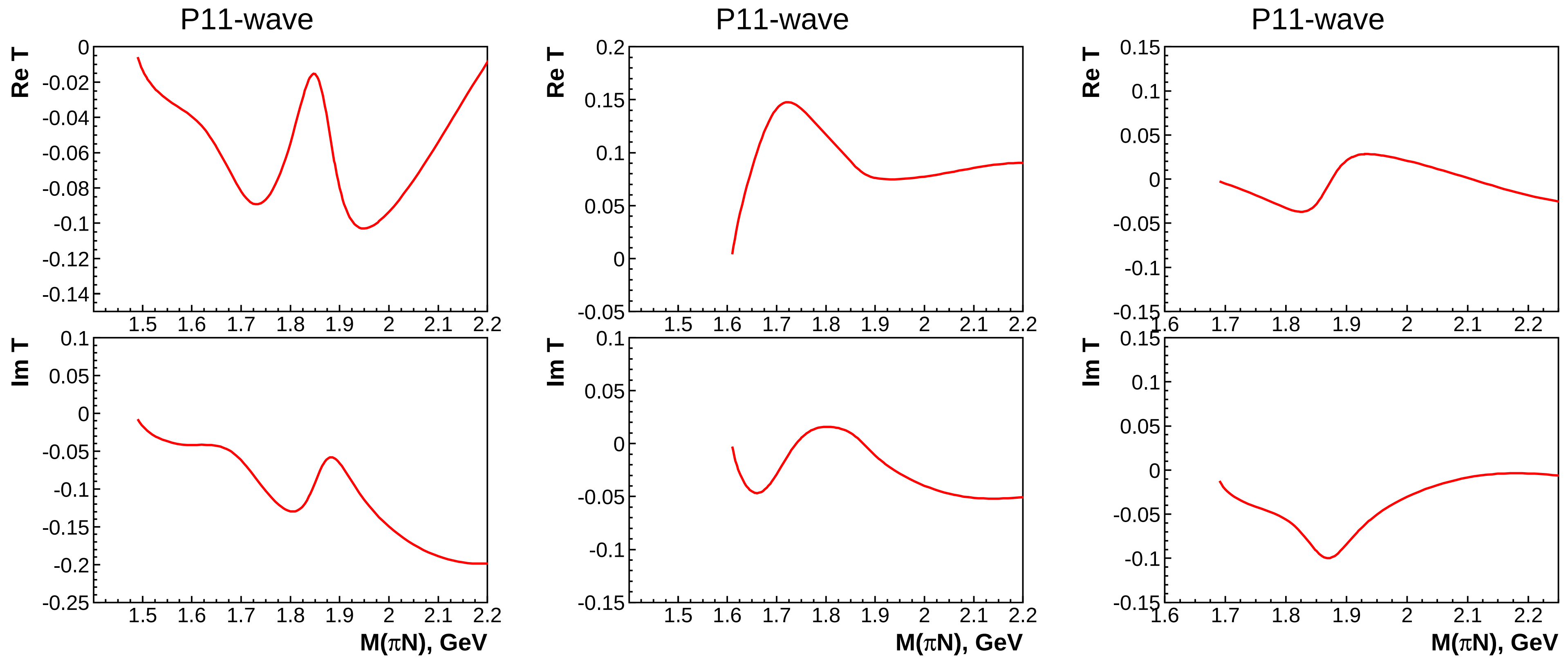

P33-wave transition amplitudes

$\pi N \to \pi N$ $\pi N \to \pi\Delta(1232)$ $\pi N \to K\Sigma$

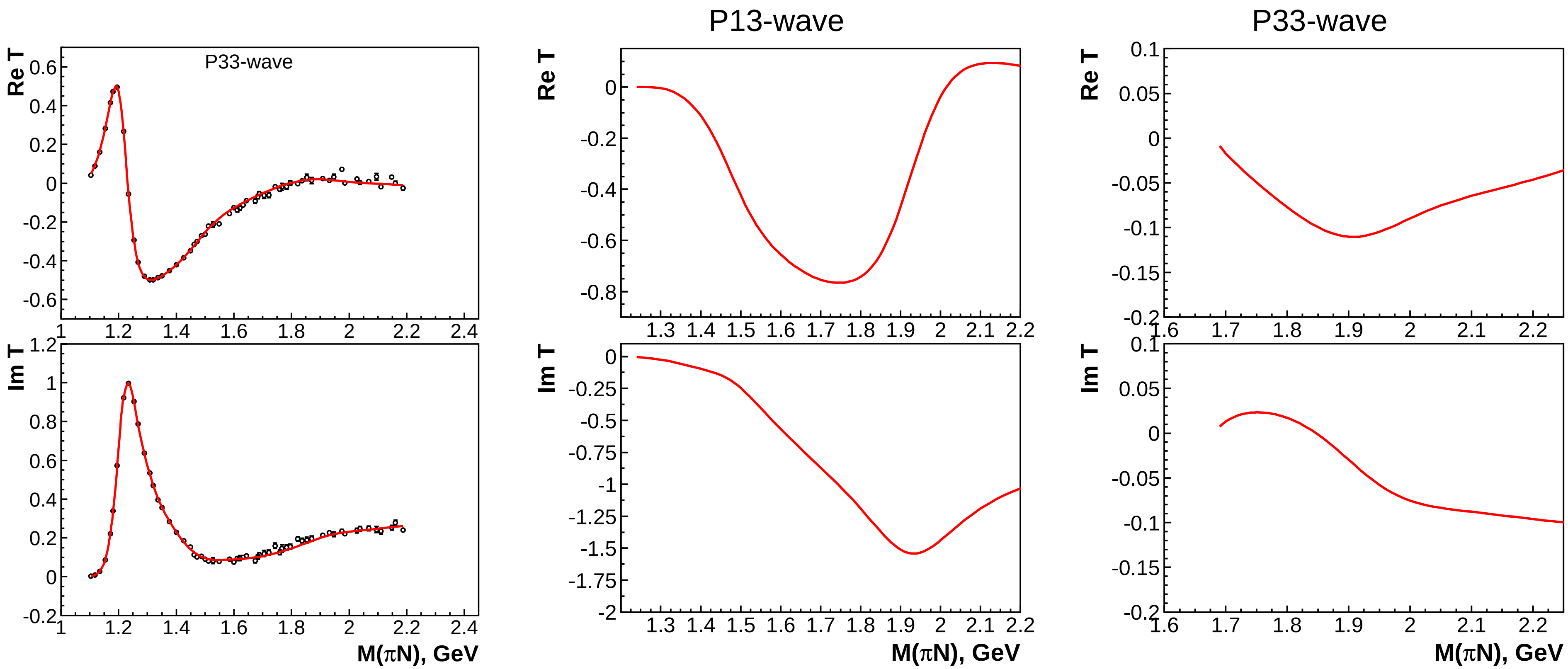

Multipoles for the single π^0 and η production. Red - real part, Blue - imaginary part.

Solid curves is our solution, dashed curves - SAID solution, dotted - MAID 2009.

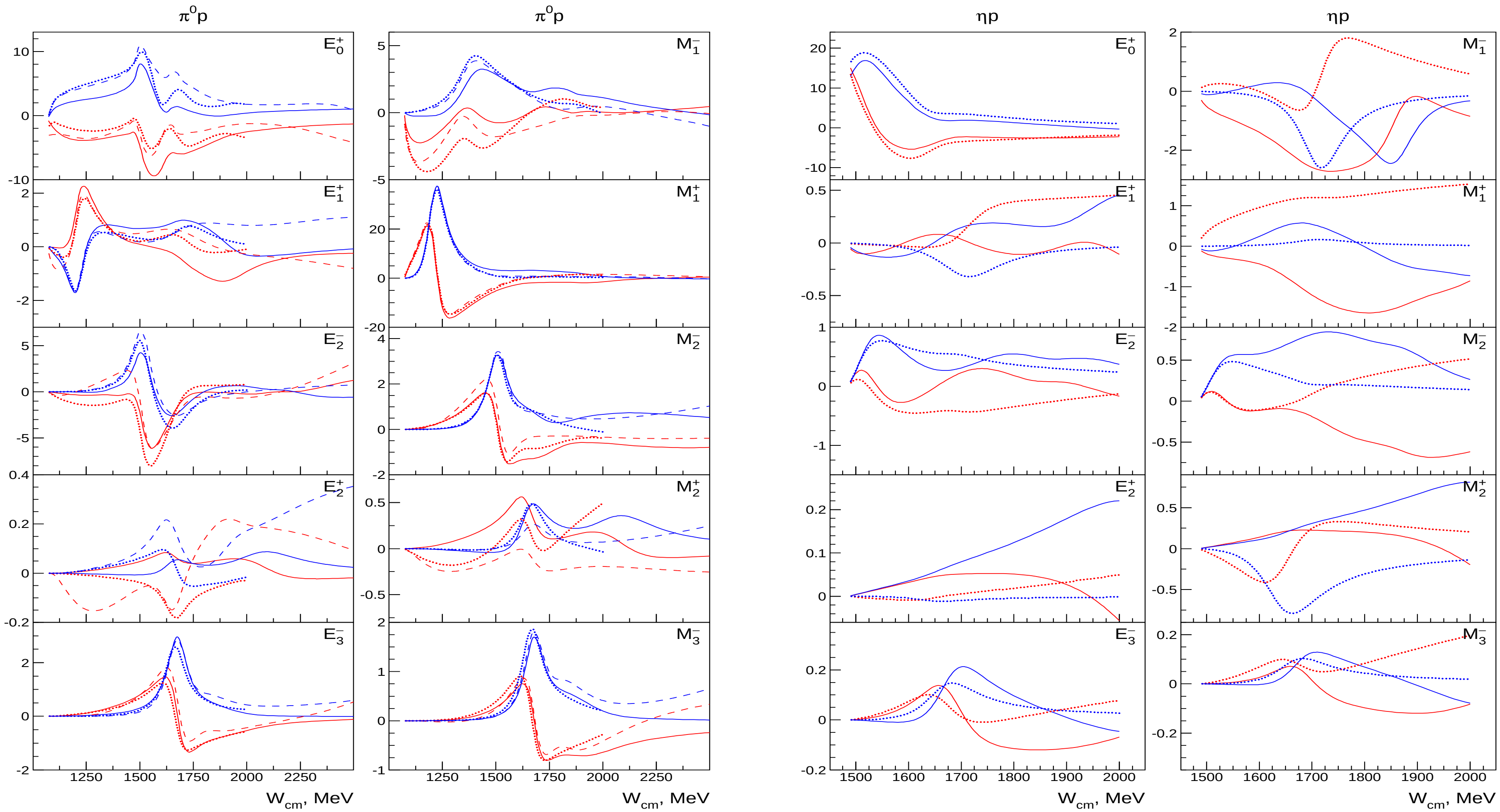

Multipoles for the $K\Lambda$ and $K\Sigma$ final states. Red - real part, Blue - imaginary part. Solid curves is our solution, dashed curves - - MAID 2009.

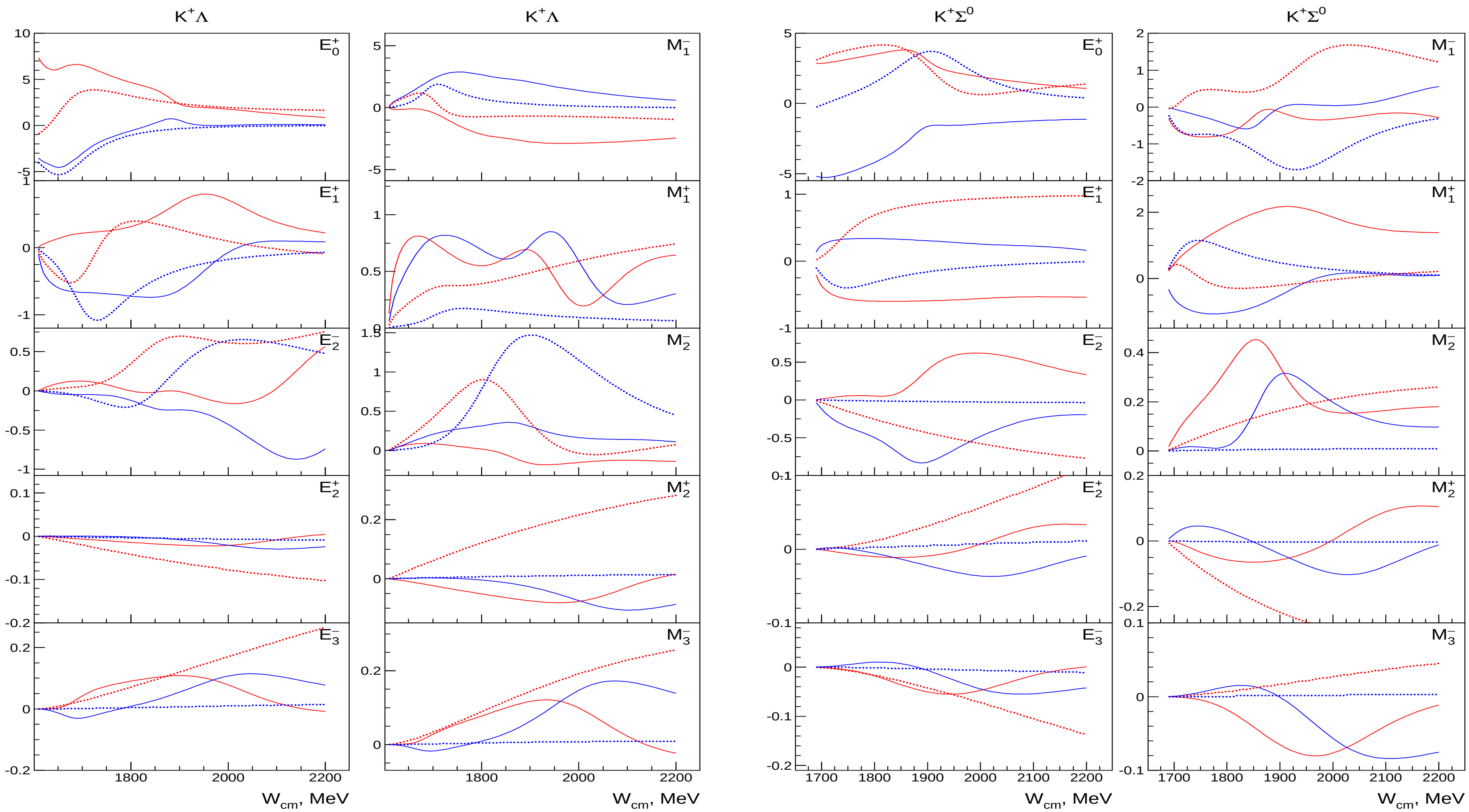

Tabelle 1: Pole position (in MeV), πN, ηN, $K\Lambda$ and $K\Sigma$ couplings (in GeV) and photo-couplings (in GeV$^{-1/2}10^3$).

State	$P_{11}(1440)$	$P_{11}(1710)$
Re(pole)	1375 ± 6 **(**1365 ± 15**)**	1690^{+25}_{-10} **(**1720 ± 50**)**
-2Im(pole)	200 ± 10 **(** 190 ± 30**)**	230^{+30}_{-20} **(** 230 ± 150**)**
$g(\pi N)$	0.49 ± 0.03 **/**-40 ± 6^o	0.16 ± 0.06 **/**-$(5^{+20}_{-50})^o$
$g(\eta N)$	-0.12 ± 0.05 **/** 20 ± 10^o	-0.16 ± 0.05 **/**-20 ± 25^o
$g(K\Lambda)$		0.70 ± 0.20 **/**-8 ± 10^o
$g(K\Sigma)$		0.10 ± 0.05 **/**$(60^{+60}_{-30})^o$
$A^{1/2}(\gamma p)$	-44 ± 10 **/**-$37^o\pm10^o$	-65 ± 25 **/** $-65^o\pm20^o$
State	$P_{11}(1840)$	$P_{13}(1720)$
Re(pole)	1860 ± 10 **( )**	1720 ± 50 **(**1675 ± 15**)**
-2Im(pole)	110^{+30}_{-10} **( )**	420 ± 80 **(**190 ± 85**)**
$g(\pi N)$	0.12 ± 0.04 **/** $(15^{+15}_{-25})^o$	0.78 ± 0.12 **/**-35 ± 10^o
$g(\eta N)$	-0.46 ± 0.10 **/** 25 ± 12^o	0.75 ± 0.15 **/**-15 ± 10^o
$g(K\Lambda)$	-$(0.07^{+0.10}_{-0.05})$ **/** $0^{+12}_{-22}{}^o$	0.60 ± 0.35 **/**-15 ± 20^o
$g(K\Sigma)$	0.30 ± 0.10 **/** $40^{+60}_{-30}{}^o$	1.15 ± 0.60 **/**-10 ± 10^o
$A^{1/2}(\gamma p)$	-14 ± 6 **/**$50^o\pm50^0$	160 ± 30 **/**-$25^o\pm35^o$
$A^{3/2}(\gamma p)$		150 ± 60 **/**$50^o\pm40^o$

Tabelle 2: Pole position (in MeV), πN, ηN, $K\Lambda$ and $K\Sigma$ couplings (in GeV) and photo-couplings (in GeV$^{-1/2}10^3$).

State	$P_{13}(1960)$	$P_{13}(1900)$
Re(pole)	$1970{\pm}12$ (∼1900)	$1890{\pm}50$ ( )
-2Im(pole)	$300{\pm}60$ ( )	270^{+200}_{-100} ( )
$g(\pi N)$	$0.13{\pm}0.20$ / $20{\pm}50^o$	$0.15{\pm}0.10$ / $(20^{+50}_{-100})^o$
$g(\eta N)$	-$0.70{\pm}0.20$ / $5{\pm}15^o$	-$(0.40^{+0.40}_{-0.30}$ /-$(5^{+70}_{-50})^o$
$g(K\Lambda)$	-$(1.10^{+0.50}_{-0.30})$ / $0{\pm}15^o$	-$0.70{\pm}0.35$ / $(5^{+70}_{-35})^o$
$g(K\Sigma)$	-$0.40{\pm}0.15$ / $(35^{+15}_{30})^o$	$0.40^{+0.50}_{-0.25}$ /-$(5^{+40}_{-100})^o$
$A^{1/2}(\gamma p)$	$9{\pm}7$ /-$2{\pm}10^o$	$63{\pm}20$ / $65^o{\pm}20^o$
$A^{3/2}(\gamma p)$	$50{\pm}40$ / $55^o{\pm}40^o$	$63{\pm}15$ / $80^o{\pm}30^o$
State	$P_{33}(1600)$	$P_{33}(1920)$
Re(pole)	$1480{\pm}40$ $(1600{\pm}100)$	$1925{\pm}40$ $(1900{\pm}50)$
-2Im(pole)	$230{\pm}40$ $(300{\pm}100)$	$320{\pm}50$ $(300{\pm}100)$
$g(\pi N)$	$0.40{\pm}0.10$ / $85{\pm}15^o$	$0.45{\pm}0.15$ /-$30{\pm}25^o$
$g(K\Sigma)$	-$0.15{\pm}0.08$ /-$15{\pm}15^o$	-$0.20{\pm}0.10$ / $20{\pm}15^o$
$A^{1/2}(\gamma p)$	$20{\pm}12$ / $55^o{\pm}20^o$	$100{\pm}20$ /-$55^o{\pm}15^o$
$A^{3/2}(\gamma p)$	$14{\pm}10$ /-$5^o{\pm}20^o$	-$73{\pm}12$ / $35^o{\pm}15^o$